

ABSTRACT

Title of Thesis: MODELING HYDRODYNAMICS AND
SEDIMENT TRANSPORT IN BALTIMORE
HARBOR: TIME-VARYING BOUNDARY
CONDITIONS

Zhenghua Jin, Master of Science, 2004

Thesis Directed By: Professor William Boicourt
Marine, Estuarine and Environmental Sciences
Program

Hydrodynamics and sediment transport under time-varying boundary conditions at Baltimore Harbor mouth are simulated using a three-dimensional model. The model predictions are compared to those produced by constant monthly-averaged salinity and sediment boundary conditions and observational data at sampling sites. For monthly average values, both model predictions are compared reasonably with observations. For short-term predictions, the model results under time-varying boundary conditions have more variability than those under constant boundary conditions, as expected. However, time-varying boundary conditions do not improve the short-term predictions significantly and much of the variability that appears in the observational data is not captured. This behavior is partially because the time-varying salinity and sediment boundary conditions are derived from CH3D model output instead of real data.

MODELING HYDRODYNAMICS AND SEDIMENT TRANSPORT IN
BALTIMORE HARBOR: TIME-VARYING BOUNDARY CONDITIONS

By

Zhenghua Jin

Thesis submitted to the Faculty of the Graduate School of the
University of Maryland, College Park, in partial fulfillment
of the requirements for the degree of
Master of Science
2004

Advisory Committee:

Professor William Boicourt, Chair
Professor Larry Sanford
Professor Shenn-yu Chao

© Copyright by
Zhenghua Jin
2004

Acknowledgements

I wish to express my gratitude to my advisor Dr. Bill Boicourt for his support, patience and advise during this study. I am also grateful to my committee members Dr. Larry Sanford and Dr. Shenn-Yu Chao. Thanks to Dr. Sanford for his valuable advises on CHARM sediment model, analysis of model results and interpolation method. Thanks to Dr. Chao for his guidance in numerical modeling. Special thanks to Dr. Harry Wang at Virginia Institute of Marine Science for providing me the CH3D model output. This study benefits a lot from the post-processor created by Steve Suttles. I am really thankful for his help. I also appreciate the support from my former advisor Dr. Leonard Walstad for my first-year study at University of Maryland. I wish to acknowledge Dr. James Carter for granding me the access to the computer facilities in Department of Meteorology.

This study could not be completed without the support and understanding from Nauth Panday, Dr. MiaoLi Chang and Lee Currey at Maryland Department of the Environment.

I also want to thank my husband and my parents for their support and encouragement during the entire study.

Table of Contents

Acknowledgements	ii
Table of Contents	iii
List of Tables	iv
List of Figures	v
List of Abbreviations	vii
Chapter 1: Introduction	1
1.1 The challenge of modeling sediment transport in Baltimore Harbor	1
1.2 Hydrodynamics and sediment transport in Baltimore Harbor - an overview	3
1.3 Objectives	8
Chapter 2: Methodology	10
2.1 Formulation of the hydrodynamic model	10
2.1.1 Introduction	10
2.1.2 Basic equations	12
2.1.3 Vertical boundary conditions	14
2.1.4 Horizontal boundary conditions	14
2.2 Formulation of the sediment transport model	15
2.2.1 Introduction	15
2.2.2 Basic equations	15
2.2.3 Boundary conditions	16
2.3 Model specifics	17
2.4 Open boundary conditions	20
2.4.1 Non-point source and point source	20
2.4.2 Salinity and sediment concentration at Harbor mouth open boundary	21
Chapter 3: Results	27
3.1 Introduction	27
3.2 Comparison of open boundary conditions at Harbor mouth	29
3.3 Mass balance checks	39
3.4 Model-data comparison	43
Chapter 4: Discussion and Conclusion	66
References	75

List of Tables

Table 3.2.1: Comparison of constant and mean value of time-varying salinity and sediment concentration at model boundary cell (51,21) near to mooring site 1	34
Table 3.2.2: Comparison of salinity and sediment concentration differences under constant and time-varying boundary conditions at mooring site 1 and sampling site 2 for CHARM 2 and CHARM 3 periods	38
Table 3.3.1: Mass balance comparison for CHARM 2 case	40
Table 3.3.2: Mass balance comparison for CHARM 3 case	41
Table 3.4.1: Mean values and standard deviations of salinity, TSS and Velocity at mooring site 1 for CHARM 2 and CHARM 3 periods	51
Table 3.4.2: Mean values and standard deviations of velocity at mooring site 1 for CHARM 3 Period	62

List of Figures

Figure 1.1.1: Study Area – Baltimore Harbor with the monitoring stations marked.....	2
Figure 2.1.1: Model grid and internal sources	11
Figure 2.4.1: CH3D Model grid in Baltimore Harbor (highlighted cells are the Harbor mouth cells and dark dots are monitoring stations)	22
Figure 2.4.2: Time series of salinity profiles at Harbor mouth (CHARM 2):01	23
Figure 2.4.3: Time series of salinity profiles at Harbor mouth(CHARM 2):02	24
Figure 2.4.4: Constant salinity distribution at Harbor mouth used in constant BC model for CHARM 2 period	26
Figure 3.1.1: Mooring site 1(47,21) and sampling site 2 (20,30) at Baltimore Harbor...	28
Figure 3.2.1: Time series (in hour) comparison of salinity at model boundary cell (51,21; near mooring site 1) for constant and time-varying boundary conditions during CHARM 2 period.....	30
Figure 3.2.2: Time series (in hour) comparison of salinity at model boundary cell (51,21; near mooring site 1) for constant and time -varying boundary conditions during CHARM 3 period.....	31
Figure 3.2.3: Time series (in hour) comparison of sediment concentration (mg/L) at model boundary cell (51,21; near mooring site 1) for constant and time-varying boundary conditions during CHARM 2 period	32
Figure 3.2.4: Time series (in hour) comparison of sediment concentration (mg/L) at model boundary cell (51,21; near mooring site 1) for constant and time-varying boundary conditions during CHARM 3 period	33
Figure 3.2.5: Time-series (in hour) of salinity and sediment concentration at mooring sites 1 surface layer under constant and time-varying boundary conditions	36
Figure 3.4.1: Model-data comparisons for TSS (A) and salinity (B) at mooring site 1 surface layer – CHARM 2	44
Figure 3.4.2: Model-data comparisons for TSS (A) and salinity (B) at mooring site 1 bottom layer – CHARM 2.....	45
Figure 3.4.3: Model-data comparisons for TSS (A) and salinity (B) at mooring site 1 surface layer – CHARM 3	46
Figure 3.4.4: Model-data comparisons for TSS (A) and salinity (B) at mooring site 1 bottom layer – CHARM 3.....	47
Figure 3.4.5: Model and data comparison of velocity at mooring site 1 bottom layer - CHARM 2.....	48
Figure 3.4.6: Model and data comparison of velocity at mooring site 1 bottom layer - CHARM 3.....	49
Figure 3.4.7: Model-data comparisons for TSS (A) and salinity (B) at sampling site 2 surface layer – CHARM 2	52
Figure 3.4.8: Model-data comparisons for TSS (A) and salinity (B) at sampling site 2 middle layer – CHARM 2.....	53
Figure 3.4.9: Model-data comparisons for TSS (A) and salinity (B) at sampling site 2 bottom layer – CHARM 2.....	54

Figure 3.4.10: Model-data comparisons for TSS (A) and salinity (B) at sampling site 2 surface layer – CHARM 3	55
Figure 3.4.11: Model-data comparisons for TSS (A) and salinity (B) at sampling site 2 middle layer – CHARM 3.....	56
Figure 3.4.12: Model-data comparisons for TSS (A) and salinity (B) at sampling site 2 middle layer – CHARM 3.....	57
Figure 3.4.13: Model axial velocity - ADCP velocity comparison at mooring site 1 surface layer – CHARM 3	58
Figure 3.4.14: Model axial velocity - ADCP velocity comparison at mooring site 1 middle layer – CHARM 3.....	59
Figure 3.4.15: Model axial velocity - ADCP velocity comparison at mooring site 1 bottom layer – CHARM 3.....	60
Figure 3.4.16: Mean velocity profiles at mooring site 1: Model predictions vs ADCP data	63
Figure 3.4.17: Model and real bathymetries at cross section of Baltimore harbor mouth	64

List of Abbreviations

CHARM: Comprehensive Harbor Assessment and Regional Modeling

CH3D: Three-dimensional Curvilinear Hydrodynamic Model

POM: Princeton Ocean Model

TSS: Total Suspended Sediment

VIMS: Virginia Institute of Marine Science

CTD: Conductivity, Salinity and Depth

ADCP: Acoustic Doppler Current Profiler

Chapter 1: Introduction

1.1 The challenge of modeling sediment transport in Baltimore Harbor

Sediment and water transport are important to water quality because sediment is a sorbing surface for chemicals and chemicals move with water currents. Many water-borne organic and inorganic chemicals exist both in dissolved form and forms sorbed to solids. The distribution between dissolved and sorbed chemicals affects the transport and fate of the contaminants in the water column and in the bottom sediments.

Baltimore Harbor is a tributary embayment located on the western side of upper Chesapeake Bay (Figure 1.1.1). Baltimore Harbor has been industrialized for a long time. As a result, Baltimore Harbor has received a myriad of contaminants (Lin et al., 2004). The Chesapeake Bay Program has designated Baltimore Harbor as one of three “Regions of Concern” in the Bay watershed where toxic pollution has resulted in significant sediment contamination, water pollution or damaged to aquatic life (Greer and Terlizzi 1997).

In order to better understand the fate of sediment-bound contaminants in Baltimore Harbor, it is necessary to investigate the mechanisms of sediment transport. Sediment transport is very complex, related to many hydrodynamic, chemical, biological and benthic processes. The largest inventory of toxic contaminants in Baltimore Harbor is in the bottom sediment. The existing inventory of contaminated sediments in the Harbor makes it difficult to regulate new inputs to the Harbor, since it is not known how much

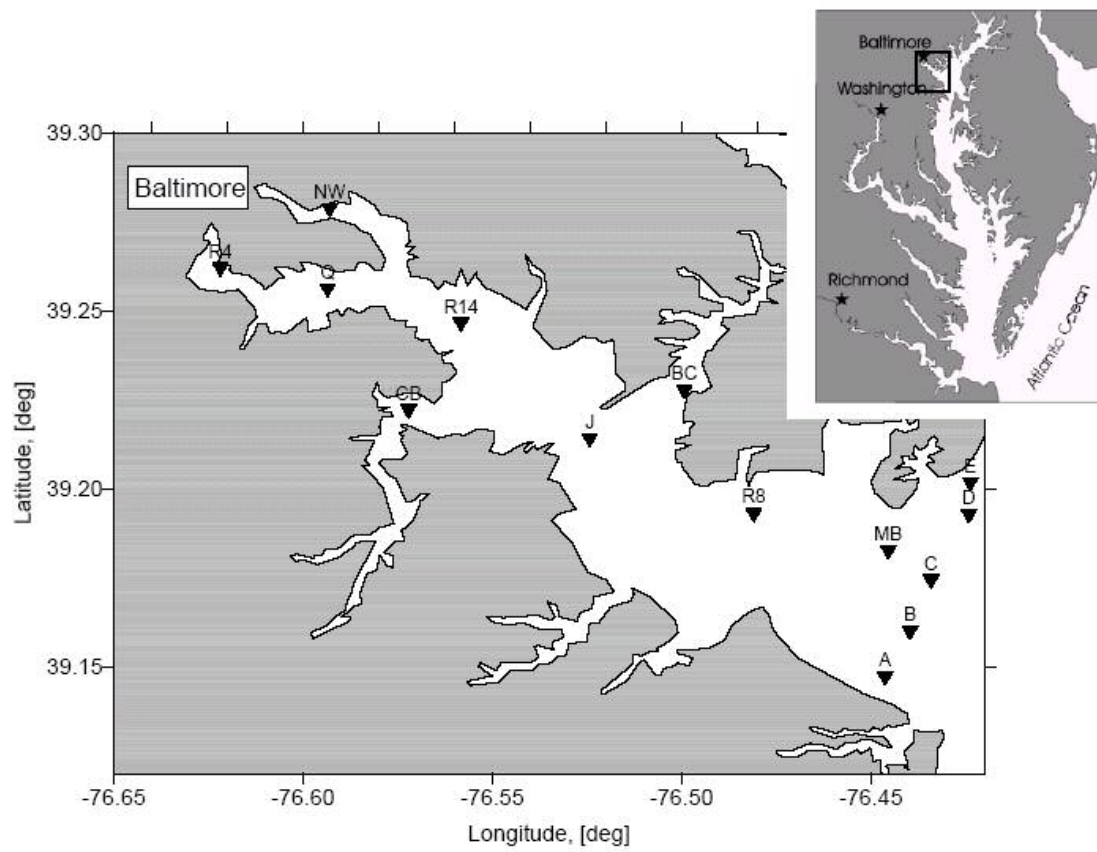


Figure 1.1.1: Study Area – Baltimore Harbor with the monitoring stations marked

these new inputs contribute to water quality problems compared to the contribution of in-place sediments.

Fortunately, there have been many investigations on the sediment transport in Baltimore Harbor in recent years. With a lot of valuable monitoring data and a well-developed hydrodynamic model (Chao, et al., 1995), Sanford et al. (1997,1999,2003) developed a sediment transport model which gave a reasonable simulation for monthly average sediment process in Baltimore Harbor. However, the latest version of this model uses constant boundary conditions at Harbor mouth and cannot capture the short-term variability in the observational data. In order to solve this problem and make a better simulation of the sediment transport in Baltimore Harbor, a quantitative model that applies time-varying boundary conditions at Harbor mouth is needed.

1.2 Hydrodynamics and sediment transport in Baltimore Harbor - an overview

Baltimore Harbor is part of the 27-km tidal portion of the lower Patapsco River (Figure 1.1.1). Natural water depths in the Harbor are generally less than 6 meters except for the main navigation channel maintained by the U.S. Army Corps of Engineers at the depth of 15 meters. The tidal range in the Harbor is approximately 0.3 meters. The only other sizable streams that enter the Harbor directly are Jones Falls and Gwynns Falls.

Previous studies of Baltimore Harbor have focused on its circulation pattern. The earliest comprehensive report (Garland, 1952) concluded water circulation and exchange within the region are generally regulated by local wind forces which overwhelm the currents driven by river and tidal forces. Based on salinity and dye studies, Pritchard and Carpenter (1960) inferred the existence of a three-layered circulation with inflows in

surface and bottom layers and outflow in middle layer in Baltimore Harbor. Later, direct long-term flow measurements were conducted in 1978-1979 (Boicourt and Olson, 1982) mainly in the deep channel of the Harbor. To verify the three-layer circulation, current data were averaged over long periods to partially remove meteorologically and tidally induced circulations. The results indicated that the three-layer circulation was persistent, but variable. The surface inflow at the top two meters of the water column is not well sampled and therefore appears to be elusive, often being masked by meteorologically driven noise. The outflow at mid-depth could be as large as 5 cm/s, often extending to the bottom and overwhelming the bottom inflow. Moreover, Patapsco River freshets could, on occasion, produce conditions in which the three-layer circulation transitions to the classical two-layer estuarine circulation. For the wind-driven circulation inside Baltimore Harbor, results showed that wind events are generally episodic over short time intervals (2-10 days). In fall and winter months, winds are prevailing northwesterly or northerly. In summer months, the prevailing winds are southwesterly. The wind-driven circulation often dominates other circulation components over short time intervals, and is particularly prominent near the head of the Harbor (Middle Branch) and in the three principal tributaries (Northwest Branch, Curtis Creek, and Bear Creek).

In recent decades, numerical models have become a powerful tool to simulate the circulation and sediment transport in estuaries and oceans. Chao et al. (1996) examined the characteristics of the three-layer circulation in reverse estuaries using a three dimensional primitive-equation model with a free surface. They found that driven by an upper-layer density deficit and low-layer density surplus from the adjacent Bay, circulation in an estuarine embayment may be three-layered, with top and bottom inflows

separated by a mid-layer outflow. This type of circulation is characterized by density forcing, background stratification and lateral depth variation in the embayment. This study showed the importance of bottom intrusion in regulating the three layer circulation. A strong or deeper upper density deficit from the adjacent Bay, bottom stress and narrowing estuary width at depths all produce transients discouraging the development of the bottom intrusion. In time, the bottom inflow invariably gains strength and thickness and squeezes up the core of the mid-layer outflow to above the mid-depth.

The largest inventory of toxic contaminants in Baltimore Harbor is in the bottom sediments, such that exposure and transport of sediment-bound contaminants is a major area of concern for environmental managers (Maryland Department of the Environment, 1996). To better understand the sediment transport characteristics in Baltimore Harbor, many studies have been conducted in recent years.

Maa et al. (1998) made in situ measurements of sediment resuspension and erosion rate. This data showed a very rapid increase in erosion resistance with depth into the sediment and apparently spatial differences in erodibility within Baltimore Harbor. This result makes it very clear that, until now, no erosion formulation has been capable of incorporating the full complexity of the erosion data set in a straightforward manner. So simplified erosion formulation was often used in later modeling studies in Baltimore Harbor.

Over the past several years, the University of Maryland Center for Environmental Science has conducted field surveys to characterize circulation, salinity, and suspended sediment conditions in Baltimore Harbor as part of Comprehensive Harbor Assessment and Regional Modeling Study (CHARM) project sponsored by Maryland Department of

the Environment. These surveys were carried out during three 1-month periods (Baker and Sanford et al., 2002). The three CHARM studies represent three distinct views of circulation and sediment dynamics in Baltimore Harbor. CHARM 1 (11 October to 8 November 1999) represents a low flow, moderate wind, fall period with very low TSS concentrations. CHARM 2 (15 March to 11 April 2000) represents a high flow, high wind early spring period with very high TSS concentrations. CHARM 3 (13 July to 10 August 2000) represents a low flow, low wind mid-summer period with intermediate TSS concentrations. Together with the May 1995 observations described in Sanford et al. (1997), these field studies represent a broad range of environmental conditions across which to evaluate sediment transport and fate.

Based on these survey observations, the CHARM hydrodynamic and sediment model was developed to simulate the circulation and sediment transport in Baltimore Harbor. The CHARM hydrodynamic and sediment model was based on a numerical model of circulation in Baltimore Harbor developed by Chao and Wu (1995). This model was an adaptation of the Princeton Ocean Model (POM) (Blumberg and Mellor, 1987) using Mellor-Yamada level 2.5 turbulence closure scheme, driven by constant climatological salinity at the mouth of the Harbor, observed winds, and observed tides at Ft. McHenry.

Sanford et al. (1997) modified this model by adding a single sediment component with simple erosion and deposition boundary conditions and an assumed settling velocity. This simplified sediment model concentrated on identifying basic features and phenomena associated with suspended sediment transport in the Harbor. Sanford et al. (1999) further modified the model by allowing for multiple independent sediment classes, and developing a greatly improved erosion boundary condition based on observations in

the Harbor. This sediment model allowed suspended sediment to stratify, improved the bottom friction parameterization, and developed a method for accounting for enhanced shear stress due to wind waves. Sanford et al. (1997) and Sanford et al. (1999) used outer boundary conditions, winds, and tides derived from a field program during May 1995.

Sanford et al. (2003) made a significant improvement in the CHARM sediment transport model over previous modeling efforts. The latest version of this model was tested and run under varying forcing conditions observed during the CHARM study, and used input and boundary conditions measured during all three field campaigns, in addition to May 1995. The major improvements for this model included grid refinement, smoothing of sea surface elevation forcing time series, decreases in model time steps, initialization of internal suspended sediment concentration based on observation, and application of temporally averaged, constant interior loads. This model allowed sediment concentration to temporarily take negative value to maintain the mass balance which is numerically required for this model. The model results indicated that sediment mass is conserved acceptably in all of cases run, especially after summing up over all of the sediment classes. The model predictions are reasonable with respect to expected behavior, particularly in response to wind events. Compared to field data, the CHARM sediment model is a reasonable predictor of large, monthly average transport of water in Baltimore Harbor. However, this model could not predict short-term, small scale variability very well. This is partly because the boundary conditions for this model are constants, consisting of averages of the survey observation.

1.3 Objectives

In this study, the latest version of the CHARM hydrodynamic and sediment transport model was modified by adopting time-varying salinity and sediment concentration boundary conditions instead of constant averages at the seaward open boundary at Harbor mouth. The purpose of this study was to improve the CHARM model predictions for current, salinity and suspended sediment by using time-varying boundary conditions, especially for short-term predictions. Since the CHARM model setup and boundary location at the Harbor mouth are fixed, and available observations at the Harbor mouth boundary are limited, it is impossible to develop a time-varying boundary condition based on observation which could fit in CHARM model time-step without further field surveys. Fortunately, Virginia Institute of Marine Science (VIMS) developed a CH3D hydrodynamic and sediment model in Baltimore Harbor and Upper Chesapeake Bay (Lin et al., 2004). This model was calibrated with observational data. The model output had a three-minute interval, which is short enough to form a time-varying boundary condition for the CHARM model. So in this study, the time-varying salinity and sediment boundary conditions at the Harbor mouth were derived from VIMS CH3D model output. Right now, the CH3D model output is the best available time-varying salinity and sediment data at the Harbor mouth.

A detailed comparison between model prediction and observation and model prediction using constant boundary conditions was conducted for CHARM 2 and CHARM 3 periods. Chapter 2 discusses the detailed model setup and parameters, input data from CHARM 2 and CHARM 3 field surveys, and open boundary conditions.

Model results are showed on Chapter 3 with following discussion and conclusion on Chapter 4.

Chapter 2: Methodology

In this study, I used the latest version of CHARM hydrodynamic and sediment transport model to simulate the hydrodynamics and sediment transport in Baltimore Harbor. The sediment transport model is built on the existing hydrodynamic model of Baltimore Harbor (Chao et al., 1995). The hydrodynamic model was based on an implementation of Princeton Ocean Model (POM) on a 360-meter square grid in the horizontal and a vertical stretched (sigma coordinate) grid with 6 layers. The model grid is shown on Figure 2.1.1. The detailed model formulation and description and boundary conditions are described in sections 2.1, 2.2, 2.3 and 2.4.

2.1 Formulation of the hydrodynamic model

2.1.1 Introduction

The hydrodynamic model was based on a numerical model of circulation in Baltimore Harbor developed by Chao and Wu (1995). This model was an adaptation of POM using the Mellor-Yamada level 2.5 turbulence closure scheme, driven by observed wind as well as water level and salinity at the Harbor entrance. It solves for salinity, water level and velocities in three dimensions.

Baltimore Harbor Non-Point and Point Source Inputs

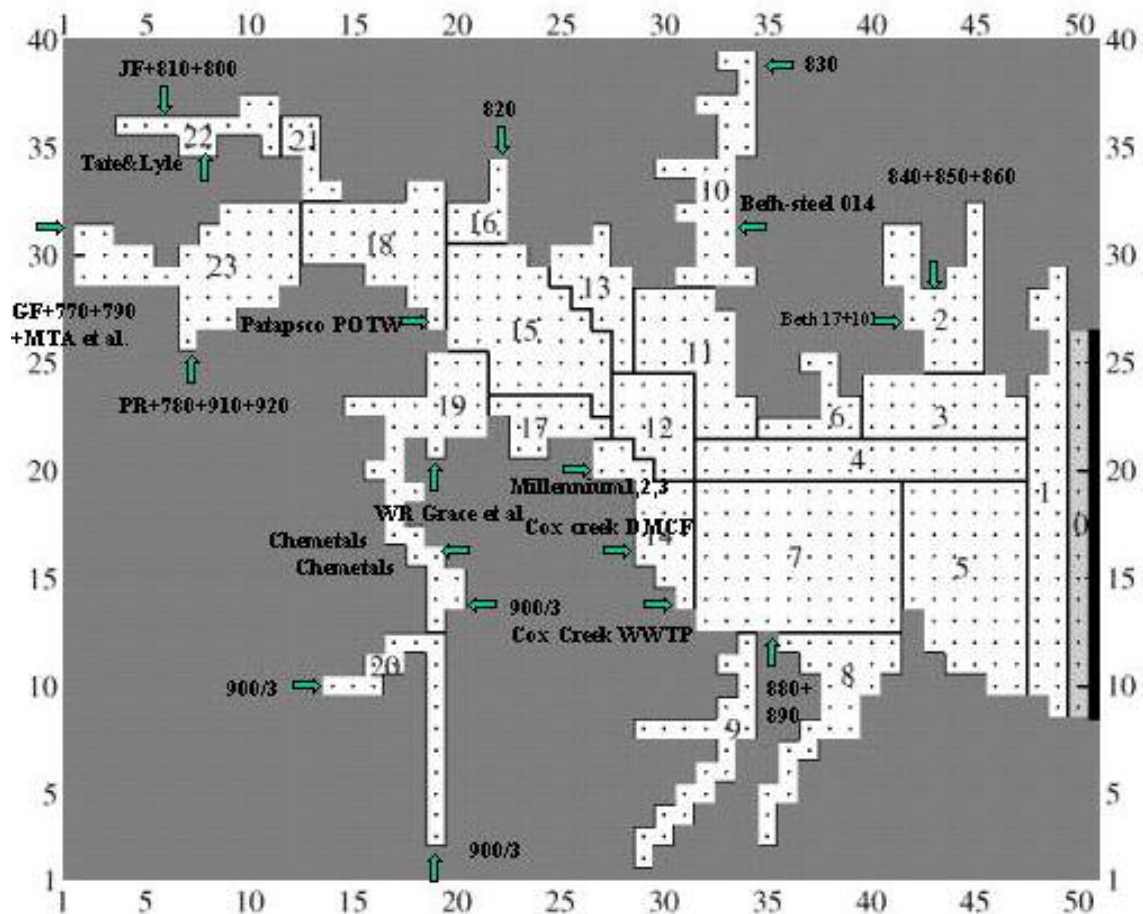


Figure 2.1.1: Model grid and internal sources

2.1.2 Basic equations

Let x, y, z be the conventional right-handed Cartesian coordinates, x and y being seaward and upward, respectively. The water is confined below by a variable bottom topography ($z = -H(x, y)$) and bounded above by a free surface ($z = \eta(x, y, t)$).

The basic equations have been cast in a bottom-following, sigma coordinate system defined by

$$\sigma = (z - \eta) / D \quad (1)$$

where $D = H + \eta$ is the local water depth. Thus, σ ranges from $\sigma = 0$ at $z = \eta$ to $\sigma = -1$ at $z = -H$.

The hydrodynamic model solves for three velocity components ((u, v, ω) in (x, y, σ) directions, respectively), free surface (η), salinity (S) and a neutrally buoyant tracer (C).

The governing equation is as followed:

$$\frac{\partial \eta}{\partial t} + \frac{\partial u D}{\partial x} + \frac{\partial v D}{\partial y} + \frac{\partial \omega}{\partial \sigma} = 0 \quad (2)$$

$$\begin{aligned} & \frac{\partial u D}{\partial t} + \frac{\partial u^2 D}{\partial x} + \frac{\partial uv D}{\partial y} + \frac{\partial u \omega}{\partial \sigma} - fv D + gD \frac{\partial \eta}{\partial x} \\ & = \frac{\partial}{\partial \sigma} \left(\frac{K_M}{D} \frac{\partial u}{\partial \sigma} \right) - \frac{gD^2}{\rho_0} \int_{\sigma}^0 \left[\frac{\partial \rho}{\partial x} - \frac{\sigma}{D} \frac{\partial D}{\partial x} \frac{\partial \rho}{\partial \sigma} \right] d\sigma + F_x \end{aligned} \quad (3)$$

$$\begin{aligned} & \frac{\partial v D}{\partial t} + \frac{\partial uv D}{\partial x} + \frac{\partial v^2 D}{\partial y} + \frac{\partial v \omega}{\partial \sigma} + fu D + gD \frac{\partial \eta}{\partial y} \\ & = \frac{\partial}{\partial \sigma} \left(\frac{K_M}{D} \frac{\partial v}{\partial \sigma} \right) - \frac{gD^2}{\rho_0} \int_{\sigma}^0 \left[\frac{\partial \rho}{\partial y} - \frac{\sigma}{D} \frac{\partial D}{\partial y} \frac{\partial \rho}{\partial \sigma} \right] d\sigma + F_y \end{aligned} \quad (4)$$

$$\frac{\partial S D}{\partial t} + \frac{\partial S u D}{\partial x} + \frac{\partial S v D}{\partial y} + \frac{\partial S \omega}{\partial \sigma} = \frac{\partial}{\partial \sigma} \left(\frac{K_H}{D} \frac{\partial S}{\partial \sigma} \right) + F_S \quad (5)$$

$$\frac{\partial C D}{\partial t} + \frac{\partial C u D}{\partial x} + \frac{\partial C v D}{\partial y} + \frac{\partial C \omega}{\partial \sigma} = \frac{\partial}{\partial \sigma} \left(\frac{K_H}{D} \frac{\partial C}{\partial \sigma} \right) + F_C \quad (6)$$

where ρ is the water density, ρ_0 is a reference (constant) water density, f is the Coriolis parameter, g is the gravitation constant, and (K_M, K_H) are coefficients of vertical viscosity and diffusivity, respectively. The equation of state for the seawater follows that of Knudsen (1901).

The horizontal viscosity and diffusion terms are defined according to:

$$F_x = \frac{\partial}{\partial x}(D\tau_{xx}) + \frac{\partial}{\partial y}(D\tau_{xy}) \quad (7a)$$

$$F_y = \frac{\partial}{\partial x}(D\tau_{xy}) + \frac{\partial}{\partial y}(D\tau_{yy}) \quad (7b)$$

where

$$\tau_{xx} = 2A_M \frac{\partial u}{\partial x} \quad (8a)$$

$$\tau_{xy} = A_M \left(\frac{\partial u}{\partial x} + \frac{\partial v}{\partial y} \right) \quad (8b)$$

$$\tau_{yy} = 2A_M \frac{\partial v}{\partial y} \quad (8c)$$

Also,

$$F_\phi = \frac{\partial}{\partial x}(Dq_x) + \frac{\partial}{\partial y}(Dq_y) \quad (9)$$

where

$$q_x = A_H \frac{\partial \phi}{\partial x} \quad (10a)$$

$$q_y = A_H \frac{\partial \phi}{\partial y} \quad (10b)$$

and where ϕ represents S or C. Coefficients of horizontal viscosity and diffusivity (A_M and A_H) are determined by the Smagorinsky's formula.

$$(A_M, A_H) = (C_M, C_H) \Delta x \Delta y \frac{1}{2} |\nabla v + (\nabla v)^T| \quad (11)$$

where values of (C_M, C_H) like 0.1 have been commonly used in ocean model.

Coefficients of vertical viscosity and diffusivity (K_M and K_H) are determined by the local turbulence intensity level, using the 2-1/2-level turbulence closure scheme as described by Mellor and Yamada (1982).

2.1.3 Vertical boundary conditions

The vertical boundary condition on equation (2) is

$$\omega(0) = \omega(-1) = 0 \quad (12)$$

The boundary condition on equations (3) and (4) are

$$\frac{K_M}{D} \left(\frac{\partial u}{\partial \sigma}, \frac{\partial v}{\partial \sigma} \right) = (\tau_x, \tau_y) / \rho_0, \sigma = 0 \quad (13a)$$

and

$$\frac{K_M}{D} \left(\frac{\partial u}{\partial \sigma}, \frac{\partial v}{\partial \sigma} \right) = C_z (u^2 + v^2)^{1/2} (u, v), \sigma = -1 \quad (13b)$$

where (τ_x, τ_y) are wind stresses in (x, y) directions, and C_z is the dimensionless bottom drag coefficient derived from a logarithmic boundary layer and generally ranges from 0.0025 to 0.02. The boundary condition on equation (5) is

$$\frac{\partial S}{\partial \sigma} = 0, \sigma = 0 \text{ and } -1 \quad (14)$$

2.1.4 Horizontal boundary conditions

All coastline boundaries are impermeable to salinity and tracer. The boundary conditions require the velocities normal to the land be set to zero. The landward tangential velocities in the horizontal friction term are also set to zero.

The Harbor mouth boundary conditions for salinity and sediment and all the non-point source and point source inputs along the Harbor will be stated in section 2.4.

2.2 Formulation of the sediment transport model

2.2.1 Introduction

The sediment transport model runs in parallel with the hydrodynamic model with the same temporal resolution. More details about the sediment components used in this model can be found in Sanford et al. (1999).

2.2.2 Basic equations

Sediment concentration C (Kg m^{-3}) in the water column is governed by

$$\frac{\partial CD}{\partial t} + \frac{\partial CuD}{\partial x} + \frac{\partial CvD}{\partial y} + \frac{\partial Cw^*}{\partial \sigma} = \frac{\partial}{\partial x} (K_H D \frac{\partial C}{\partial x}) + \frac{\partial}{\partial y} (K_H D \frac{\partial C}{\partial y}) + \frac{\partial}{\partial \sigma} (\frac{K_V}{D} \frac{\partial C}{\partial \sigma}) \quad (1)$$

where (u, v) are fluid velocities in the (x, y) directions, D is local water depth, K_H is the horizontal eddy diffusivity and K_V is the vertical eddy diffusivity. The vertical motion of the sediment is accompanied by a settling velocity (w_s), so that $w^* = W - w_s$, where W is the vertical fluid velocity. The vertical eddy diffusivity (K_V) is determined by the local turbulence intensity, using the 2.5-level turbulent closure scheme described by Mellor and Yamada (1982). Density stratification damping of K_V in the present model includes the effect of suspended sediment stratification (Chao, 1998), by including the effect of suspended sediment in the calculation of the water density:

$$\rho_c = \rho + (1 - \rho_0 / \rho_s)C \quad (2)$$

where the density of clear seawater (ρ) is a function of salinity and pressure, ρ_0 is a reference density of clear seawater, and ρ_s is the density of fully compacted sediments, assuming there is no space between particles. Horizontally, K_H is determined by the Smagorinsky's first-order closure scheme,

$$K_H = 0.1\Delta x\Delta y \frac{1}{2} |\nabla v + (\nabla v)^T| \quad (3)$$

where $\Delta x = \Delta y = 360\text{m}$.

2.2.3 Boundary conditions

Boundary conditions for the suspended sediment concentration are as follows. At the water surface, no sediment flux is allowed, so that

$$w_s CD + K_v \frac{\partial C}{\partial \sigma} = 0 \quad (4)$$

At the bottom, sediment flux is the difference between the deposition rate (D_E) and erosion rate (E), so that

$$w_s C + K_v \frac{\partial C}{\partial \sigma D} = D_E - E \quad (5)$$

In this study, D_E and E are using the same formulations as used in the latest version of CHARM sediment model. The detail descriptions can be found in Sanford et al. (1999).

On side walls, sediment flux normal to the boundary is zero, so that

$$\frac{\partial C}{\partial n} = 0 \quad (6)$$

where n is normal to the boundaries.

At the Harbor mouth, the sediment flux is dictated by advection, so that

$$\frac{\partial C}{\partial t} + u_n \frac{\partial C}{\partial n} = 0 \quad (7)$$

where u_n is the velocity normal to the open boundary. The implementation of (7) on the open boundary requires the knowledge of C values at grid point spacing outside the computation domain. These boundary values are provided by the model output from CH3D Upper Chesapeake Bay sediment model developed by Lin and Wang (Lin et al., 2004), apportioned appropriately by settling class, which is stated in section 2.4.

2.3 Model specifics

In this study, the main purpose is to see what difference it will bring to the hydrodynamics and sediment transport process in Baltimore Harbor by different kind of open boundary conditions at Harbor mouth. The former model was driven by constant salinity and sediment concentration at Harbor mouth and the present model was driven by the time-varying salinity and sediment concentration at Harbor mouth. Two field surveys with extreme meteorological data among CHARM and 1995 field studies were chosen for this study – CHARM 2 and CHARM 3. CHARM 2 (15 March to 11 April 2000) represents a high flow, high wind early spring period with very high TSS concentrations. CHARM 3 (13 July to 11 August 2000) represents a low flow, low wind mid-summer period with intermediate TSS concentrations.

The hydrodynamic and sediment transport models of Baltimore Harbor were run over 60 day time periods, starting 14 February 00am to 14 April 00am 2000 For CHARM 2 and starting 14 June 00am to 13 August 00am 2000 for CHARM 3. The model was allowed to spin up during the first 30 days of the 60-day run, storing only the last 30 days of model output for comparison with field data.

Two different versions of the model were configured to make up a complete sediment transport run, based on particle settling speed. The particle settling speeds chosen were based on settling tube observations in the Harbor. They comprised intermediate settling particles (0.3 mm/s), and slow settling particles (0.007 mm/s). Simulations with a non-settling tracer (referred to as the dissolved cases below) were also run, initializing the Harbor waters with zero sediment concentration and maintaining a constant open boundary sediment concentration of 0.001. Each version of the sediment transport model was initialized by extrapolating the monthly averaged channel observations of their respective total suspended sediment (TSS) concentrations laterally across the Harbor, greatly shortening the spin-up time for suspended sediment predictions. These suspended conditions were applied 10 days after the hydrodynamic model was started, and 20 days before the period of interested began.

The external mode (for calculation of sea surface height and associated currents) used a two second time step for dissolved and slow cases and one second time step for intermediate cases, and the internal mode (for calculation of salinity, mixing and baroclinic currents) used eight second time step for dissolved and slow cases and four second time step for intermediate cases.

The wind time series were developed using Thomas Point Light wind data for the entire running periods. The sea level elevation forcing was changing at discrete (6 min) intervals and the values were from interpolated observations. Tidal elevation time series at the Harbor mouth were developed based on the linear interpolation of observations between Tolchester Beach (39.21°N, 76.25°W) in Chesapeake Bay and Ft. McHenry

(39.27°N, 76.58°W) inside Baltimore Harbor. Temperature was assumed to be constant at 20 deg C.

Bottom stress was calculated assuming a quadratic drag formulation with a drag coefficient set as the maximum of the equivalent to a bottom roughness of 0.01m or 0.001. This formulation was only applied to the first modeled velocity point above bottom. The height of this velocity point changes from location to location due to the vertical σ coordination system.

Surface wave are known to be an important forcing for sediment resuspension in the shallow upper Chesapeake Bay (Sanford 1994). Nakagawa et al (2000) showed that spatial distributions of sand fraction in Baltimore Harbor sediments are quite well correlated with model-estimated extreme wave forcing. Surface wave induced bottom stress was included in the sediment transport model by running the steady state wave model HISWA for 4 different wind speeds and 16 different wind directions with the same grid spacing as the circulation model. Predicted wave-induced bottom velocities were stored at each grid point of the circulation model for each combination of wind speed and direction, then were accessed and interpolated during the sediment transport model runs, converted to shear stresses using a drag coefficient of 0.03, and vectorially added to the circulation induced skin friction values. This combined bottom stress was used to calculate sediment erosion rate in each grid cell.

Fine sediment erosion was modeled following Sanford and Maa (2001), based on data collected in Baltimore Harbor by J. Maa as described in Maa et al. (1998). The average erodibility characteristics of all the sites occupied were used to describe erosion of a pure Harbor mud, and the erosion rate was then decreased as necessary in each model cell to

account for any sand fraction present based on Harbor sediment mapping data. Importantly, the sediment transport model didn't allow for modification of the sediment bed through winnowing of fine sediment or new deposition. Fine sediment deposition was modeled as the product of the component sediment settling velocity and a reference deposition concentration near the bottom. The reference concentration was calculated using a method that ensures no dependence on the thickness of the model grid cells. The deposition of suspended sediment is disallowed during periods of erosion.

2.4 Open boundary conditions

2.4.1 Non-point source and point source

The model included interior Harbor fresh water and sediment sources. These interior sources include both non-point source (three major rivers and watershed flow/loadings) and point sources (industrial and municipal facilities). The locations of all these point and non-point sources are indicated in Figure 2.1.1. For each source, the model opened one more cell to represent it. For these boundary cells, the sea level elevations and water depths were set to be the same as the cells next to it. The horizontal velocity normal to the flow direction and vertical velocity were set to zero. The horizontal velocities in the flow direction and sediment concentration were applied as temporally averaged, constant values at the 6 vertical layers for each input location. The sediment loads were applied as 50% intermediate settling and 50% slow settling particles. The flow and sediment load information were derived through a combination of watershed modeling and data analysis.

2.4.2 Salinity and sediment concentration at Harbor mouth open boundary

The salinity and sediment concentration boundary conditions at Harbor mouth were derived from the model output of CH3D hydrodynamic and sediment model developed for upper Chesapeake Bay (Lin et al., 2004). The CH3D model salinity and sediment concentration output has a 3-minute time step for the whole study periods of CHARM 2 and CHARM 3. Ch3D model has different model grid from the model used here. Figure 2.4.1 showed the CH3D model grid around Baltimore Harbor and the highlighted cells are the cells nearest to the open boundary cells of the model used in this study and the time-varied salinity and sediment outputs in these cells were used to derived the salinity and sediment concentration in corresponding open boundary cells at Harbor mouth in this study. The dark points shown on this figure are the five monitoring stations at Harbor mouth. The boundary at Harbor mouth in this study is along these monitoring stations and shown on Figure 2.1.1 with number zero. The two boundaries are very close to each other but not completely overlaid. This study used linear interpolation/extrapolation method based on depth to derive the values of open boundary conditions at Harbor mouth from CH3D model output at a 6-minute time step. Figure 2.4.2 and Figure 2.4.3 showed time series of salinity distribution profiles at Harbor mouth using CH3D output and the salinity distribution profile at Harbor mouth using interpolated salinity data for period of CHARM 2 case. According to these figures, the two data sets showed good agreement and the interpolation method apparently worked properly to derive data from one grid system to the other. For sediment concentration, the same interpolation method was used to convert data from CH3D model output to the boundary cells of the model used in this study. For CH3D model, there are three sediment classes: clay, silt and sand. The

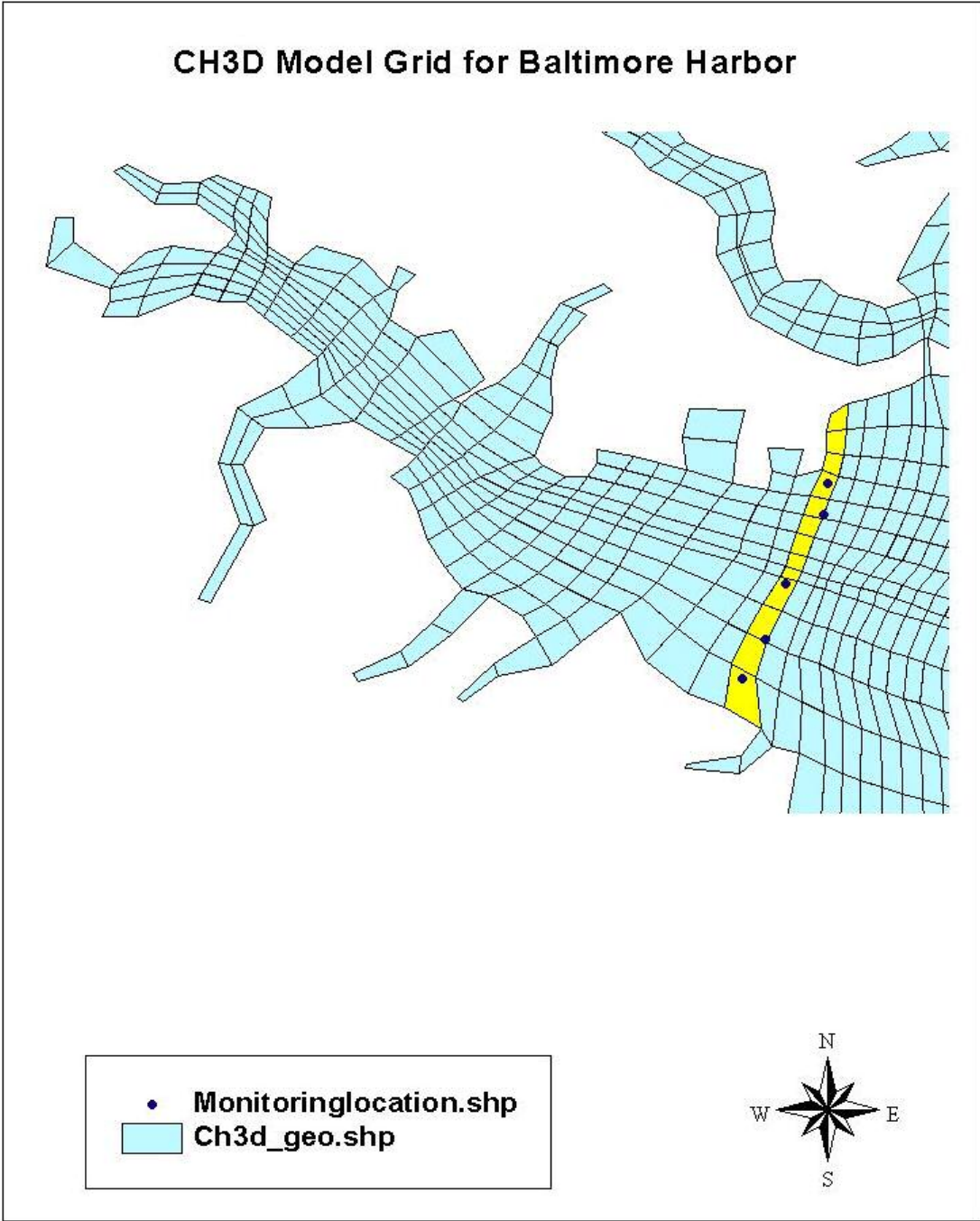


Figure 2.4.1: CH3D Model grid in Baltimore Harbor (highlighted cells are the Harbor mouth cells and dark dots are monitoring stations)

Salinity profiles at Harbor mouth
from CH3D model output

Interpolated salinity profile at Harbor
mouth for CHARM model

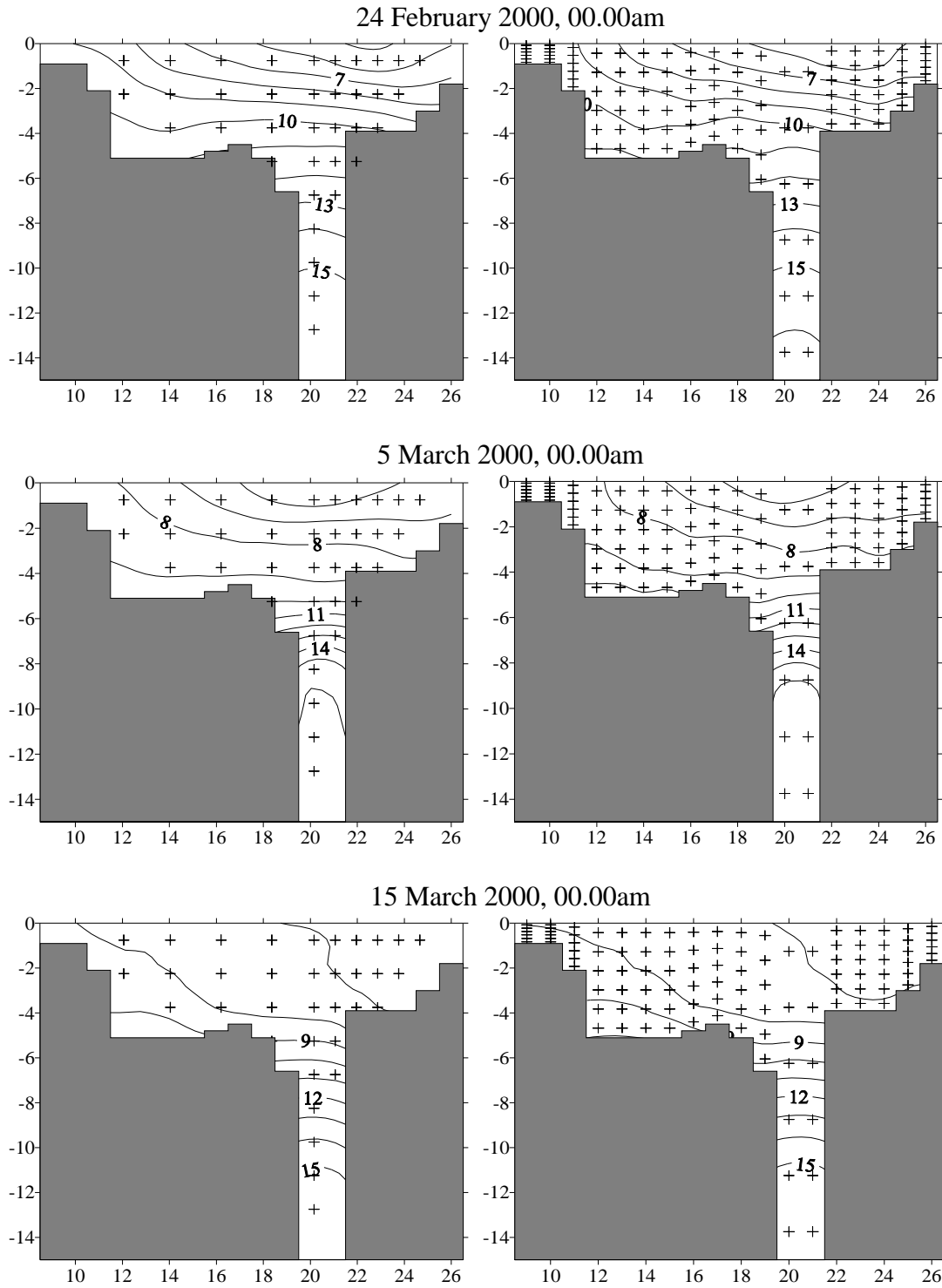


Figure 2.4.2: Time series of salinity profiles at Harbor mouth (CHARM 2):01
 (“+” signs are the model grids for CH3D(left) or CHARM model(right))

Salinity profiles at Harbor mouth
from CH3D model output

Interpolated salinity profile at Harbor
mouth for CHARM model

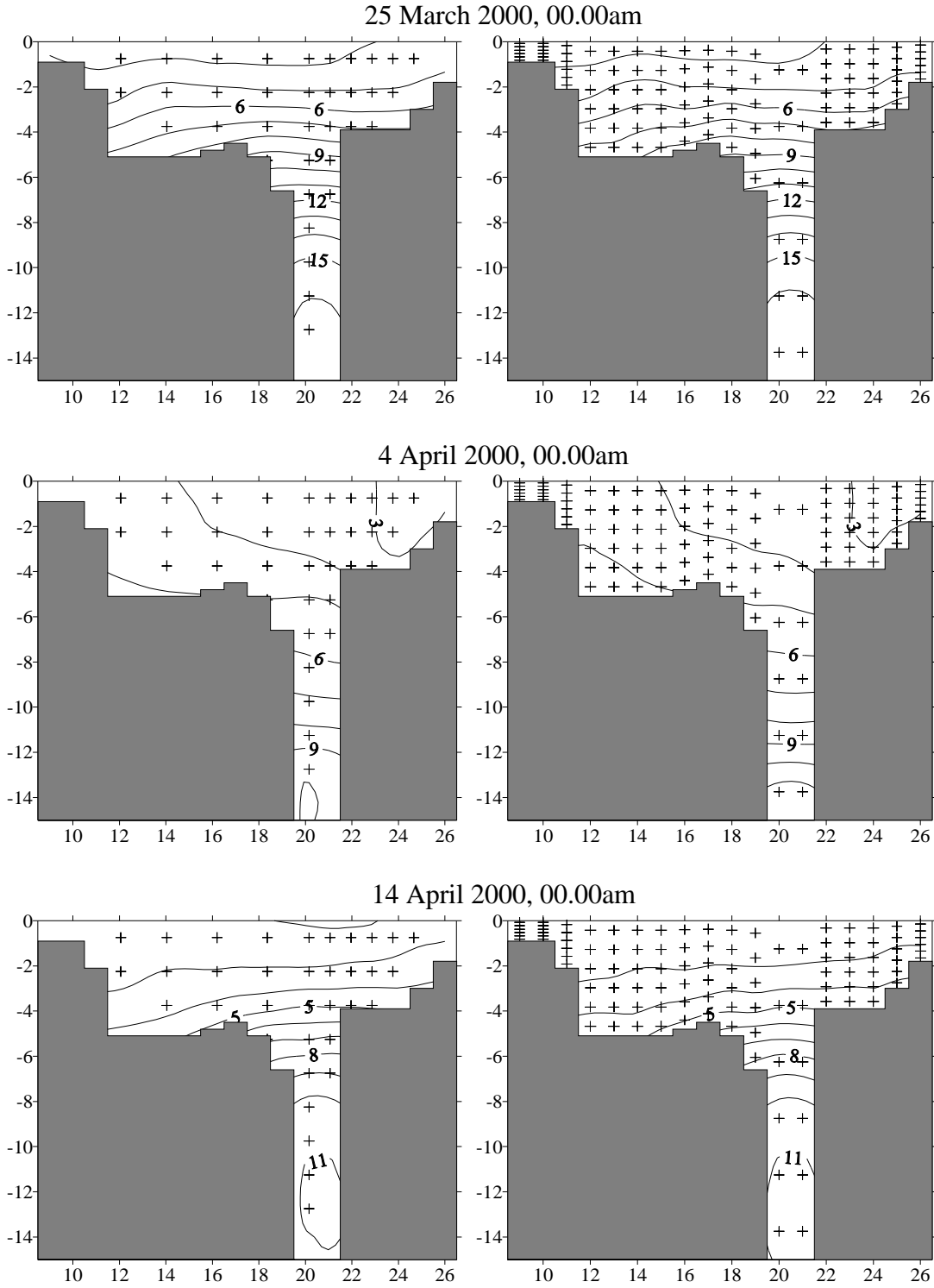


Figure 2.4.3: Time series of salinity profiles at Harbor mouth(CHARM 2):02
 (“+” signs are the model grids for CH3D(left) or CHARM model(right))

diameters of the three sediment classes are represented by 3.5, 15 and 65 μm , and the initial settling velocities are 0.01 mm/s, 0.7 mm/s and 3.3 mm/s, respectively (Lin et al., 2004). According to the settling velocities of these three classes, the sediment concentration of clay was used as sediment input in slow settling case, and those of silt and sand were added together as sediment input in intermediate settling case in the model used in this study. The model updated salinity and sediment concentration at Harbor mouth boundary every 6 minutes.

The constant salinity and sediment concentrations at the Harbor mouth boundary are the monthly averaged values interpolated from the monitoring data. The constant salinity boundary condition distribution at the Harbor mouth (Figure 2.4.4) is stratified in the vertical and homogeneous in the horizontal (the near-boundary salinity variations in Figure 2.4.4 are induced by the contour plotting process). Water in the surface layer is well mixed. For the time-varying boundary condition model used in this study, the time-varying salinity distribution at the Harbor mouth (Figure 2.4.2 and Figure 2.4.3) is stratified in the vertical, especially in the deep channel.

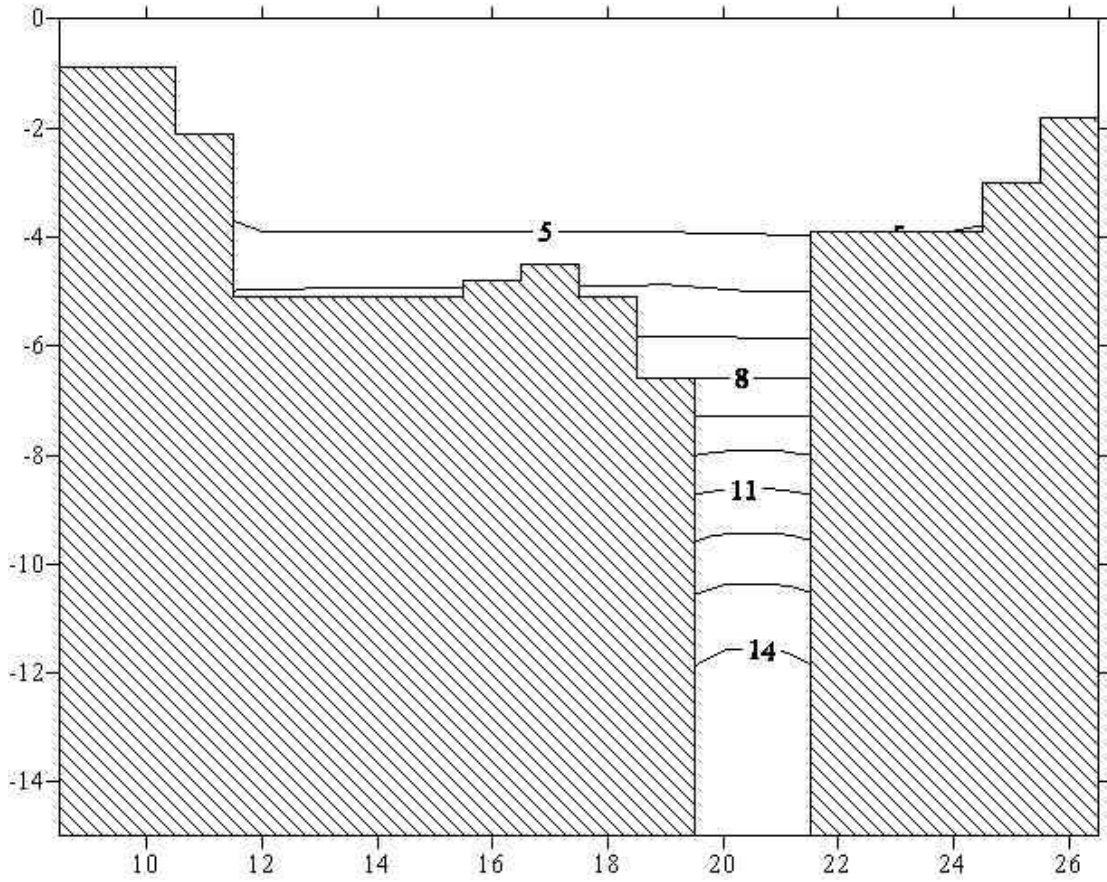


Figure 2.4.4: Constant salinity distribution at Harbor mouth used in constant boundary condition model for CHARM 2 period

Chapter 3: Results

3.1 Introduction

Model results under constant (hereafter referred to as constant BC model) and time-varying (hereafter referred to as time-varying BC model) salinity and sediment boundary conditions at Harbor mouth and observational data are compared in this chapter. There are two aspects of model-data comparison. The first, and most rigorous, is the comparison of observed time series at specific locations and times to hourly model predictions at the closest model grid cells. The short-term variability of model predictions and data will be clearly shown in this kind of comparison. The second is comparison of monthly averaged data at specific locations to monthly averaged model predictions at the closest grid cells.

Figure 3.1.1 shows the monitoring sites (respect to model grid) in Harbor used for data and model comparison in this chapter. Mooring site 1 (grid point (47,21)) is located in the deep channel and about 1.5 km from the Harbor mouth (with grid point $x = 51$). Sampling site 2 (20,30) is in the upstream part of deep channel and about 12 km from Harbor mouth. Both sites are about 16-meter deep. This study chooses CHARM 2 and CHARM 3 periods as the simulation periods because they represent the two extreme conditions in CHARM study. CHARM 2 is the most dynamic period with high flow, high wind and high TSS concentration. CHARM 3 is the calmest one with low flow, low wind and intermediate TSS concentration.

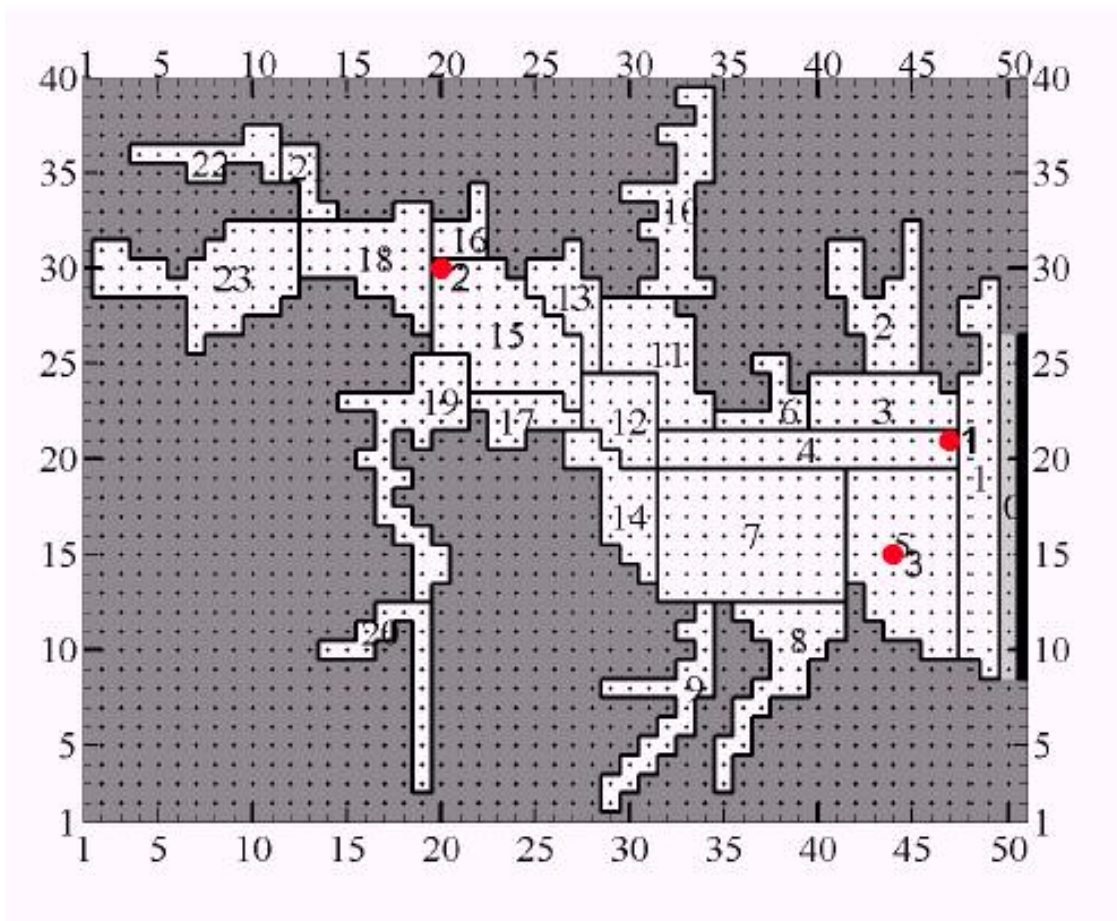


Figure 3.1.1: Mooring site 1(47,21) and sampling site 2 (20,30) at Baltimore Harbor

The results of this study are presented in sections 3.2, 3.3 and 3.4. In section 3.2, the two sets of salinity and sediment boundary conditions at Harbor mouth are compared. Also in this section, the differences of salinity and sediment concentration under two sets of boundary conditions at two monitoring sites are compared to investigate how boundary condition effects propagate along the deep channel. Mass balance and sediment mass budget results of both model predictions for CHARM 2 and CHARM 3 periods are checked in section 3.3. The mass balance was checked to ensure the model could achieve stable, mass conservative solutions. The sediment mass budget will indicate the relative importance of each process in sediment transport. Section 3.4 shows the model-data comparison of total suspended sediment (TSS) concentration, salinity and velocity at mooring site 1 and sampling site 2 for both CHARM 2 and CHARM 3 periods. These comparisons will show if the short-term predictions of CHARM model are improved under time-varying boundary conditions.

3.2 Comparison of open boundary conditions at Harbor mouth

Time-series of salinity at Harbor mouth boundary cell (51, 21) near to mooring site 1 (47,21) are shown in Figure 3.2.1 and Figure 3.2.2 for CHARM 2 and CHARM 3 periods, along with the constant salinity at Harbor mouth boundary used in constant BC model. The time-varying salinity varies around the constant salinity in nearly all cases. According to Table 3.2.1, the mean values of time-varying salinity at cell (51, 21) are close to the constant salinities used in constant BC model boundary.

Figure 3.2.3 and Figure 3.2.4 are the time series of sediment concentration at boundary cell (51,21) for CHARM 2 and CHARM 3 periods, along with the constant

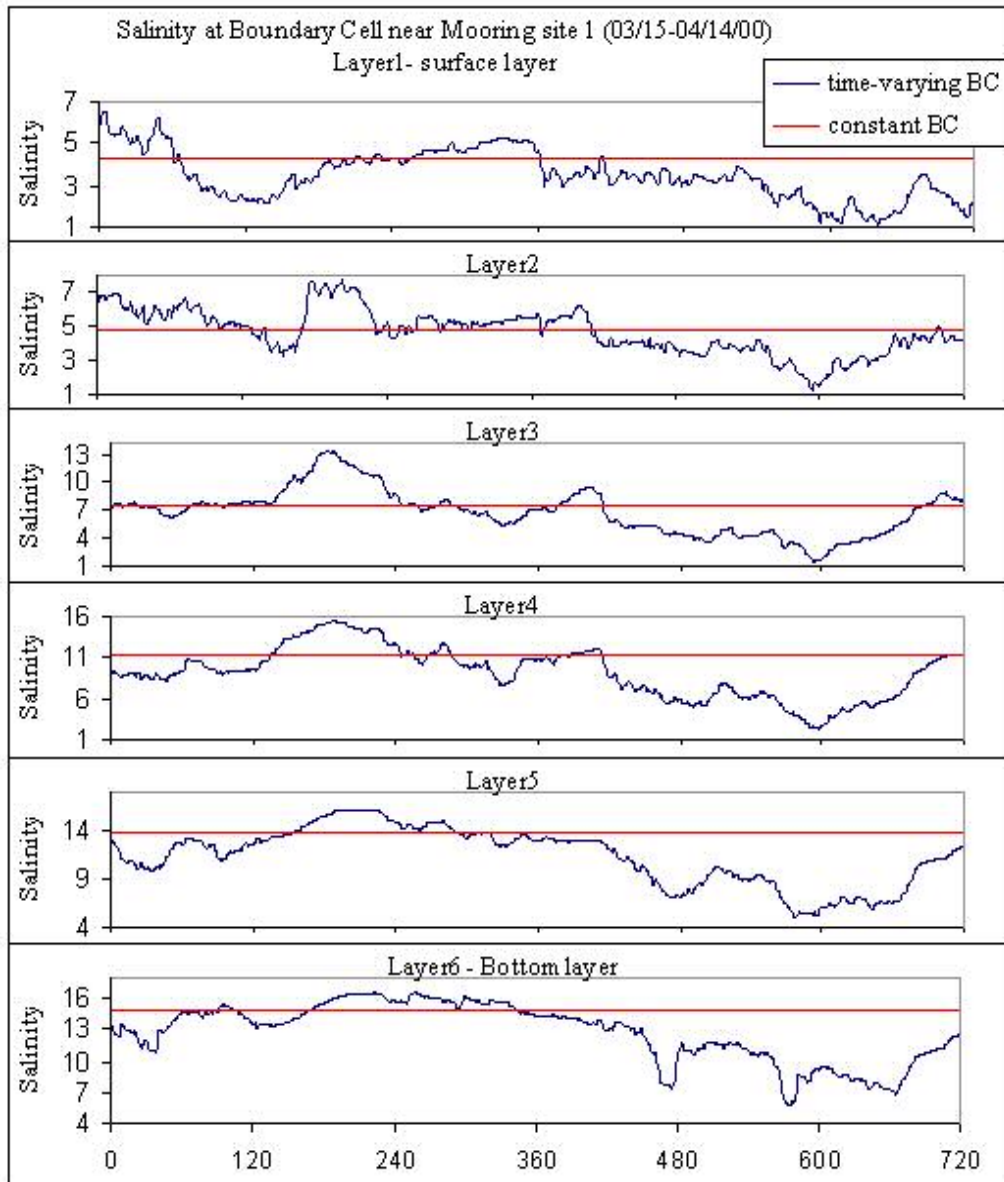


Figure 3.2.1: Time series (in hour) comparison of salinity at model boundary cell (51,21; near mooring site 1) for constant and time-varying boundary conditions during CHARM 2 period

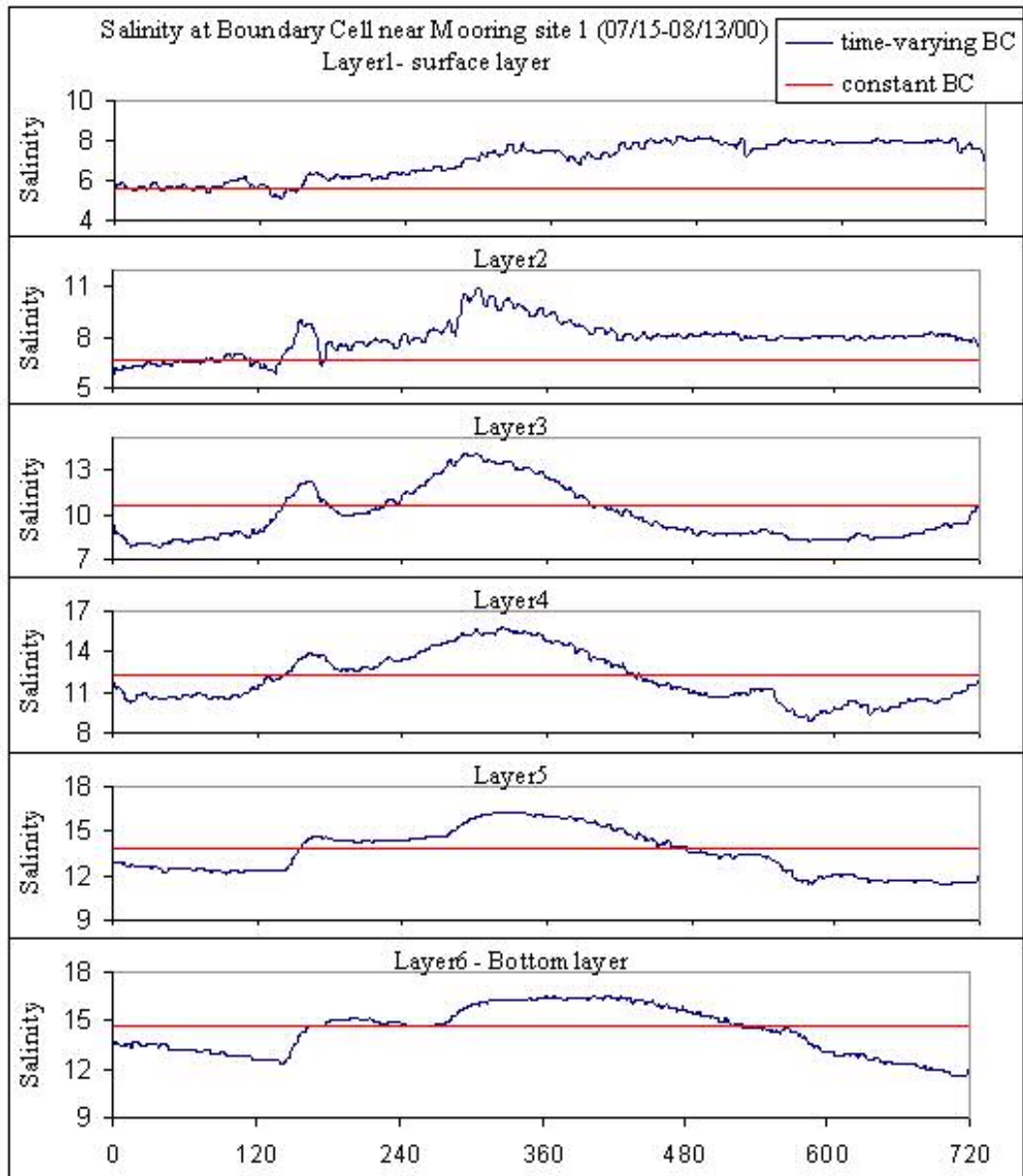


Figure 3.2.2: Time series (in hour) comparison of salinity at model boundary cell (51,21; near mooring site 1) for constant and time-varying boundary conditions during CHARM 3 period

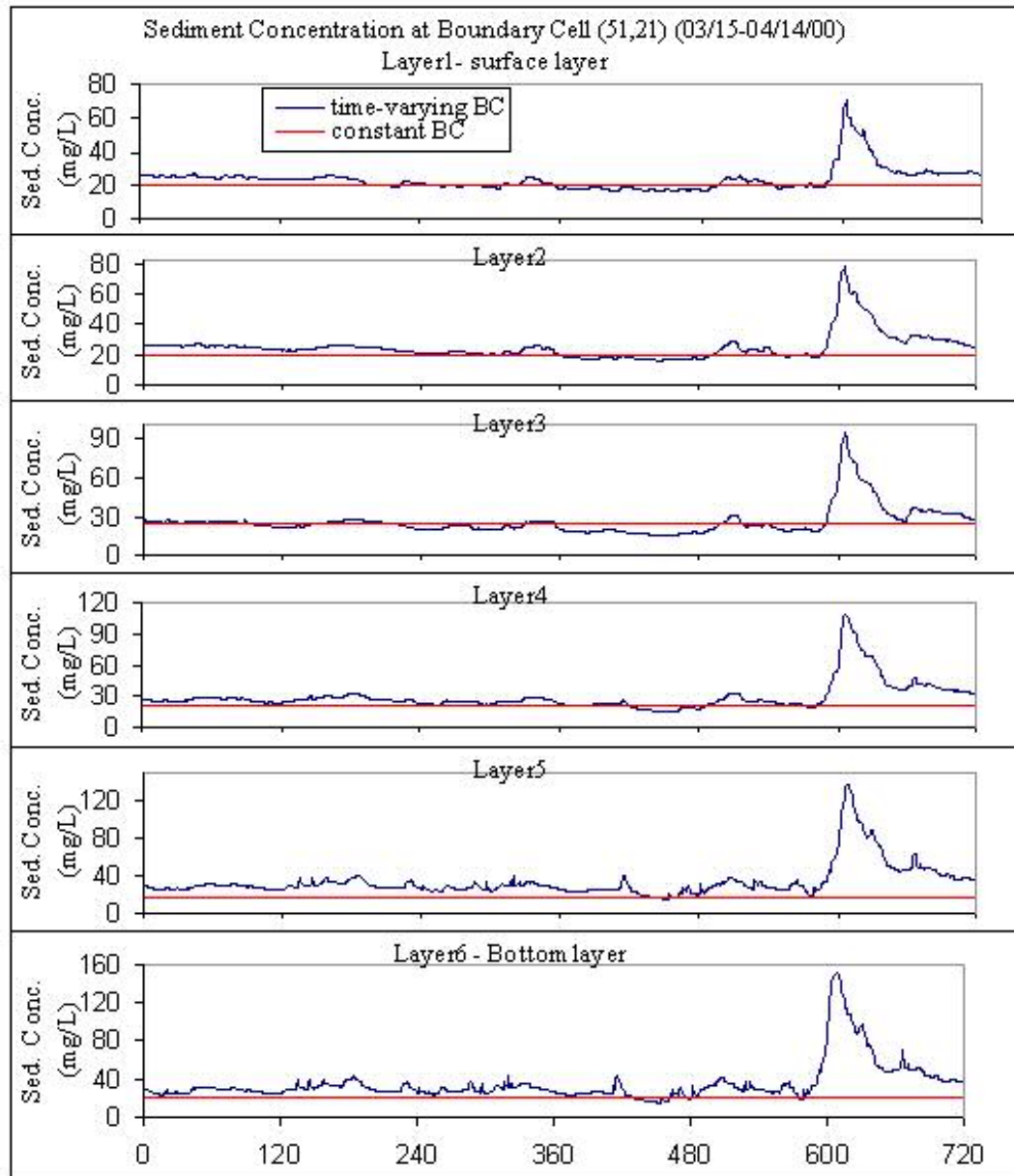


Figure 3.2.3: Time series (in hour) comparison of sediment concentration (mg/L) at model boundary cell (51,21; near mooring site 1) for constant and time-varying boundary conditions during CHARM 2 period

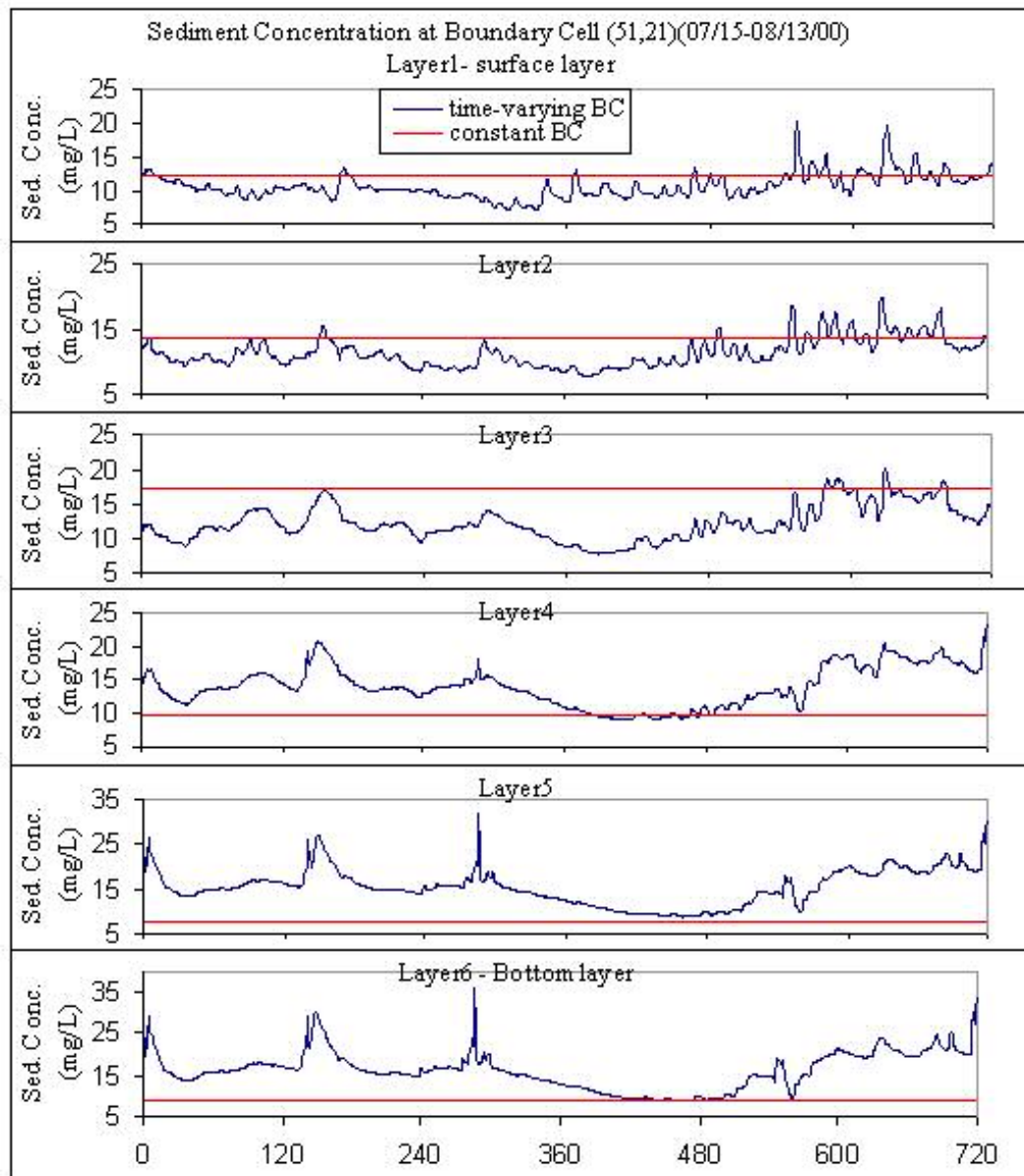


Figure 3.2.4: Time series (in hour) comparison of sediment concentration (mg/L) at model boundary cell (51,21; near mooring site 1) for constant and time-varying boundary conditions during CHARM 3 period

	Vertical layer	CHARM 2	
		Constant BC	Time-varying BC
Mean Salinity (psu)	layer 1(surface)	4.31	3.50
	layer 2	4.83	4.68
	layer 3	7.49	6.79
	layer 4	11.23	9.18
	layer 5	13.90	11.33
	layer 6(bottom)	14.93	12.73
Mean Sediment concentration (mg/L)	layer 1(surface)	20.88	23.73
	layer 2	19.88	24.78
	layer 3	24.10	25.82
	layer 4	20.51	29.15
	layer 5	16.92	33.75
	layer 6(bottom)	20.59	35.46
	Vertical layer	CHARM 3	
		Constant BC	Time-varying BC
Mean Salinity (psu)	layer 1(surface)	5.61	7.03
	layer 2	6.67	7.96
	layer 3	10.54	9.96
	layer 4	12.26	12.02
	layer 5	13.81	13.55
	layer 6(bottom)	14.63	14.36
Mean Sediment concentration (mg/L)	layer 1(surface)	12.35	10.63
	layer 2	13.51	11.33
	layer 3	17.35	12.30
	layer 4	9.69	13.83
	layer 5	7.61	15.40
	layer 6(bottom)	9.18	16.29

Table 3.2.1: Comparison of constant and mean value of time-varying salinity and sediment concentration at model boundary cell (51,21) near to mooring site 1

sediment concentration used in constant BC model. For the CHARM 2 case, the sediment concentrations at this boundary cell in time-varying BC model are near the constant sediment concentrations used in constant BC model most of the simulation period but with a large spike about 5 days before the simulation period ends. For the CHARM 3 case, in the surface layers, the sediment concentrations in this boundary cell in time-varying BC model vary around the values of constant sediment concentrations used in constant BC model. But in the bottom layers, the sediment concentrations are larger than the values of constant concentration used in constant BC model for nearly the entire simulation period of CHARM 3. As seen in Table 3.2.1, the mean values of sediment concentration are larger than constant sediment concentrations used in constant BC model at all vertical layers for CHARM 2 case due to the large spike, and in the bottom layers for CHARM 3 case.

In order to investigate how boundary condition effects propagate along the deep channel, the differences of model predictions under two sets of boundary conditions for both sampling sites were calculated and compared. I will take the salinity and sediment concentration at mooring site 1 surface layer for CHARM 2 period as an example to illustrate how to calculate the differences. Figure 3.2.5 shows the salinity and sediment concentration under both boundary conditions. It is clear that the model predictions of salinity and sediment are different under two sets of boundary conditions. But how different are they? I used the Root-Mean-Square (RMS) of model predictions under two sets of boundary conditions to measure the difference. The RMS is calculated using the following equation:

$$\text{RMS} = \sqrt{\sum (S1 - S2)^2 / N}$$

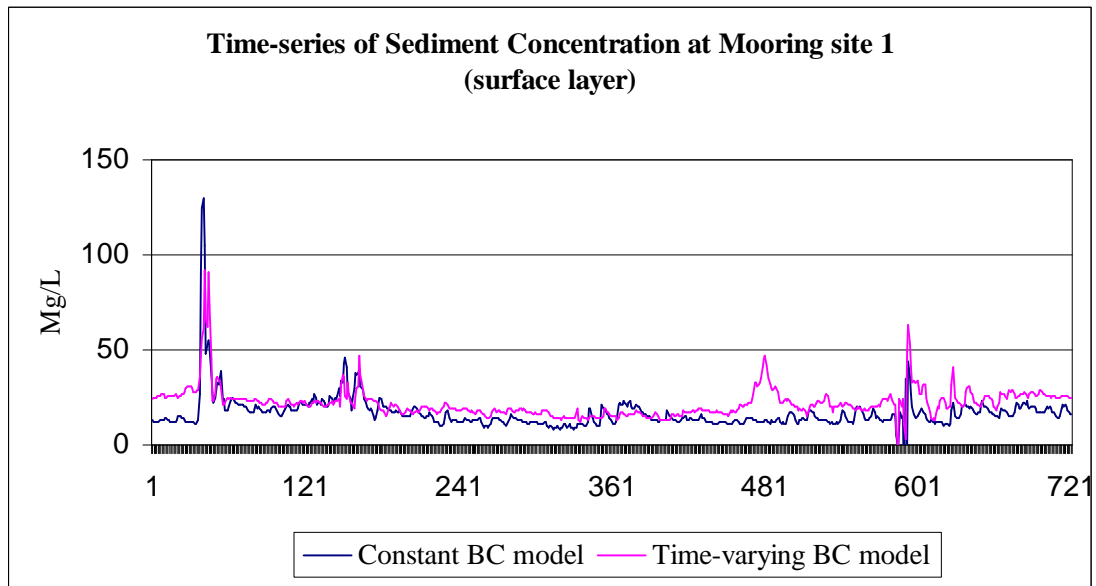
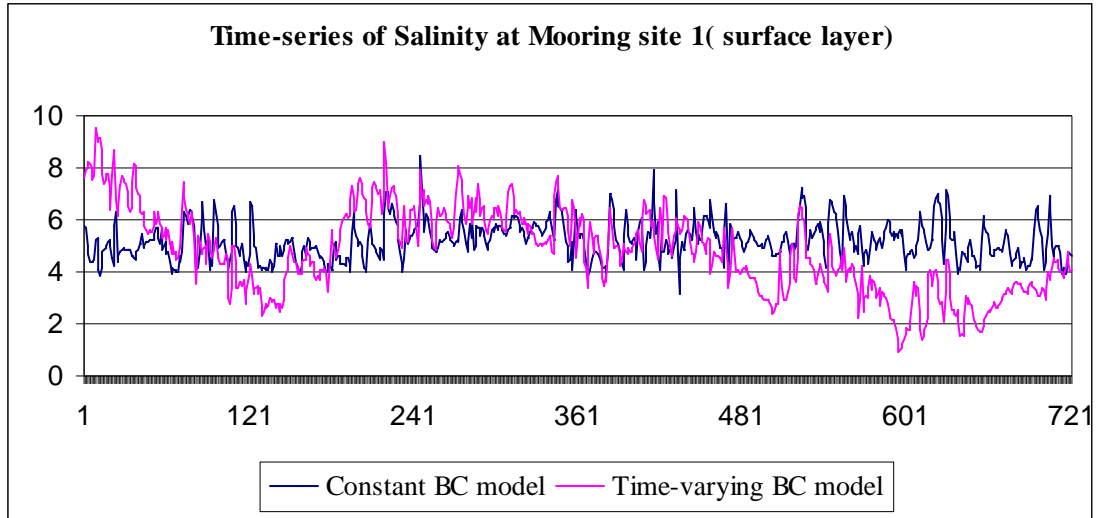


Figure 3.2.5: Time-series (in hour) of salinity and sediment concentration at mooring sites 1 surface layer under constant and time-varying boundary conditions

where S1 is the model hourly prediction under constant boundary conditions and S2 is model hourly prediction under time-varying boundary conditions at the same time. N is the total hours of calculation period. The calculated differences of salinity and sediment concentration under both sets of boundary conditions at both sampling sites are summarized in Table 3.2.2 for CHARM 2 and CHARM 3 periods. From the table, we find that, for salinity, the difference is bigger in mooring site 1 than in sampling site 2 for all cases except for the two surface layers for CHARM 2 period. Nearly all the salinity differences under two sets of boundary conditions at sampling site 2 are about more than 70% of differences at mooring site 1. For suspended sediment concentration, the differences under two sets of boundary conditions are also bigger in mooring site 1 than in sampling site 2. All the sediment concentration differences at sampling site 2 are less than 50% of those at mooring site 1. These results are consistent with the fact that mooring site 1 is closer to Harbor mouth boundary than sampling site 2. Mooring site 1 is about 1.5 km away from Harbor mouth and sampling site 2 is about 12 km from Harbor mouth. So it is reasonable that boundary conditions have more effect on model predictions at mooring site 1 than on predictions at sampling site 2. Since the salinity differences under two sets of boundary conditions do not decrease much from mooring site 1 to sampling site 2, it means that the boundary condition effects propagate efficiently into the Harbor via deep channel for salinity. But for sediment, the boundary condition effects do not propagate in deep channel as far as for salinity.

	CHARM 2			
	Salinity Difference		Sediment Conc. Difference	
	Mooring site 1	Sampling site 2	Mooring site 1	Sampling site 2
Layer 1 (surface)	1.68	1.91	9.38	4.14
Layer 2	1.71	2.02	9.15	4.22
Layer 3	2.12	2.10	8.70	4.48
Layer 4	2.86	2.20	10.44	4.95
Layer 5	3.40	2.18	12.58	5.17
Layer 6 (bottom)	3.71	2.21	14.45	5.37
	CHARM 3			
	Salinity Difference		Sediment Conc. Difference	
	Mooring site 1	Sampling site 2	Mooring site 1	Sampling site 2
Layer 1 (surface)	1.53	1.13	4.93	1.40
Layer 2	1.44	1.19	5.16	1.50
Layer 3	1.48	1.33	5.19	1.82
Layer 4	1.62	1.38	5.29	2.40
Layer 5	1.76	1.42	5.91	2.58
Layer 6 (bottom)	2.01	1.54	6.17	2.69

Table 3.2.2: Comparison of salinity and sediment concentration differences under constant and time-varying boundary conditions at mooring site 1 and sampling site 2 for CHARM 2 and CHARM 3 periods

3.3 Mass balance checks

If a model functions well, it must conserve mass balance for the simulation area. Thus, before conducting the model-data comparisons, sediment mass balance must be checked. A comparison of monthly accumulated mass balance calculation results of constant BC model and time-varying BC model are presented in Table 3.3.1 for the CHARM 2 case and Table 3.3.2 for the CHARM 3 case. The entire study area is divided into 24 boxes from box 0 at the Harbor mouth to box 23 at the head as shown in Figure 2.1.1. These calculations are based on the hourly averaged box model fluxes and TSS concentrations of model predictions. All components are reported in thousands of metric tons (10^6 kg). In descending order, the rows of each of the tables are: the total suspended sediment in the Harbor at the start time point (M_{start}); sediment mass added from internal sources including riverine inputs (Patapsco River, Jones Falls and Gwynns Falls), nonpoint sources from watershed and major point sources (M_{influx}); sediment mass imported across the open boundary at the Harbor mouth ($M_{boundaryflux}$); gross erosion of bottom sediment (M_{eroded}); gross deposition of bottom sediment ($M_{deposited}$); net erosion of bottom sediment ($M_{eroded} - M_{deposited}$); initial mass plus all additions minus all subtractions (M_{remain} : mass budget); suspended sediment mass at the last time point (M_{end}); the difference of the mass budget and the sediment mass at the last time point ($M_{remain} - M_{end}$: the absolute error); the average suspended sediment mass over the last month of simulating period (M_{ave}); and the absolute error divided by the average suspended mass times 100 (the percent error). The columns for each case represented the slow settling case, intermediate settling case, and the sum of these two components.

Constant BC model - CHARM 2

Model Run>>	BH00_slow	BH00_med	BH00_all
M_{start} (10 ⁶ kg)	4.461	0.405	4.867
M_{influx} (10 ⁶ kg)	2.480	2.480	4.960
M_{boundaryflux} (10 ⁶ kg)	12.351	-19.366	-7.016
M_{eroded} (10 ⁶ kg)	0.000	80.995	80.995
M_{deposited} (10 ⁶ kg)	14.275	64.383	78.658
M_{eroded} - M_{deposited} (10 ⁶ kg)	-14.275	16.612	2.337
M_{remain} (10 ⁶ kg)	5.017	0.131	5.148
M_{end} (10 ⁶ kg)	5.066	0.012	5.078
M_{remain} - M_{end} (10 ⁶ kg)	-0.049	0.119	0.070
M_{ave} (10 ⁶ kg)	4.822	0.887	5.709
Percent error	-1.010	13.380	1.226

Time-varying BC model - CHARM 2

Model Run>>	BH00_slow	bh00_med	BH00_all
M_{start} (10 ⁶ kg)	8.660	0.348	9.007
M_{influx} (10 ⁶ kg)	2.480	2.480	4.960
M_{boundaryflux} (10 ⁶ kg)	18.307	0.431	18.738
M_{eroded} (10 ⁶ kg)	0.000	89.077	89.077
M_{deposited} (10 ⁶ kg)	21.509	92.253	113.762
M_{eroded} - M_{deposited} (10 ⁶ kg)	-21.509	-3.176	-24.685
M_{remain} (10 ⁶ kg)	7.938	0.083	8.020
M_{end} (10 ⁶ kg)	8.004	0.021	8.025
M_{remain} - M_{end} (10 ⁶ kg)	-0.066	0.062	-0.004
M_{ave} (10 ⁶ kg)	7.221	1.131	8.352
Percent error	-0.917	5.474	-0.051

Table 3.3.1: Mass balance comparison for CHARM 2 case
(Refer to the text for the meaning of each row)

Constant BC model - CHARM 3

Model Run>>	BH00b_slow	BH00b_med	BH00b_all
M_{start} (10 ⁶ kg)	2.414	0.017	2.431
M_{influx} (10 ⁶ kg)	2.194	2.194	4.387
M_{boundaryflux} (10 ⁶ kg)	5.400	1.741	7.141
M_{eroded} (10 ⁶ kg)	0.000	10.957	10.957
M_{deposited} (10 ⁶ kg)	7.258	13.237	20.495
M_{eroded} - M_{deposited} (10 ⁶ kg)	-7.258	-2.280	-9.538
M_{remain} (10 ⁶ kg)	2.749	1.671	4.421
M_{end} (10 ⁶ kg)	2.754	1.677	4.432
M_{remain} - M_{end} (10 ⁶ kg)	-0.005	-0.006	-0.011
M_{ave} (10 ⁶ kg)	2.415	0.174	2.589
Percent error	-0.200	-3.480	-0.425

Time-varying BC model - CHARM 3

Model Run>>	BH00b_slow	BH00b_med	BH00b_all
M_{start} (10 ⁶ kg)	3.430	0.019	3.449
M_{influx} (10 ⁶ kg)	2.194	2.194	4.387
M_{boundaryflux} (10 ⁶ kg)	8.010	9.862	17.872
M_{eroded} (10 ⁶ kg)	0.000	10.292	10.292
M_{deposited} (10 ⁶ kg)	10.170	20.344	30.514
M_{eroded} - M_{deposited} (10 ⁶ kg)	-10.170	-10.052	-20.222
M_{remain} (10 ⁶ kg)	3.465	2.022	5.487
M_{end} (10 ⁶ kg)	3.478	2.014	5.492
M_{remain} - M_{end} (10 ⁶ kg)	-0.013	0.008	-0.005
M_{ave} (10 ⁶ kg)	3.338	0.210	3.548
Percent error	-0.400	3.770	-0.149

Table 3.3.2: Mass balance comparison for CHARM 3 case
(Refer to the text for the meaning of each row)

Examining the mass balance for CHARM 2 and CHARM 3 cases, it is apparent that the absolute mass balance error is always very small relative to the largest mass balance component in its respective column under both boundary conditions. For the slow settling sediment and intermediate settling sediment cases, the largest component is always the erosion or deposition term, so exchanges across the sediment-water interface dominate the mass balance of these cases. Combining these two cases together, we get the total sediment budget as a whole. For both CHARM 2 and CHARM 3 periods under both boundary conditions, the dominant process in total sediment budgets is erosion or deposition. The horizontal sediment flux through open boundary at the Harbor mouth is about one order magnitude less than erosion or deposition for dynamic CHARM 2 period and is about one third to half of erosion or deposition for calm CHARM 3 period. Compared to erosion/deposition and boundary flux, the suspended sediment in water column and sediment input from internal sources within the Harbor are relatively small.

For all the cases under constant or time-varying boundary conditions, the overall sediment percent errors are less than 1.3%, which is small enough to ensure the numerical models preserving mass balance for sediment transport. For cases under time-varying boundary conditions in this study, sediment mass balance percent errors are even smaller, less than 0.2% for the total sediment.

Comparing each item in mass balance calculation under both boundary conditions, it is obvious that boundary sediment flux across Harbor mouth from the adjacent Bay under time-varying boundary conditions is larger in all cases. This means that more sediment is imported from adjacent Chesapeake Bay under time-varying boundary conditions than under constant boundary conditions. This is because the time-varying boundary

conditions indicate a tidal “pumping effect” on the sediment transport through the Harbor mouth. I will illustrate this in detail in the discussion part. Also the erosion and deposition items for CHARM 2 period and deposition for CHARM 3 period are larger under time-varying BC model. For the total sediment of both simulation periods, the suspended sediment in water column is larger under time-varying BC model, too.

3.4 Model-data comparison

The comparisons of data and model results under constant and time-varying boundary conditions at Harbor mouth are illustrated in this section. Compared to observation, the constant BC model gave better monthly averaged predictions than short-term predictions (Sanford et al., 2003). This study focuses on the short-term predictions corresponding to time-varying salinity and sediment boundary conditions at Harbor mouth.

Figure 3.4.1 to Figure 3.4.6 show comparisons of time series data from mooring site 1, as well as periodic survey samples, with model predictions using two sets of boundary conditions at mouth. The data include TSS (total suspended sediment), salt and current velocity from an S4 current meter (resolved into the axial direction for the present purpose), for CHARM 2 and CHARM 3 periods.

In general, the model predictions under two sets of boundary conditions are different. But both models gave reasonable predictions for sediment and salt. However, even with the time-varying boundary conditions, the model still under-predicts the variability of sediment, especially near the bottom at mooring site 1. For velocity in bottom layers, the predicted velocity misses a lot of variability that apparently appears in the velocity data. The mean values and standard deviations of these data and model predictions at mooring

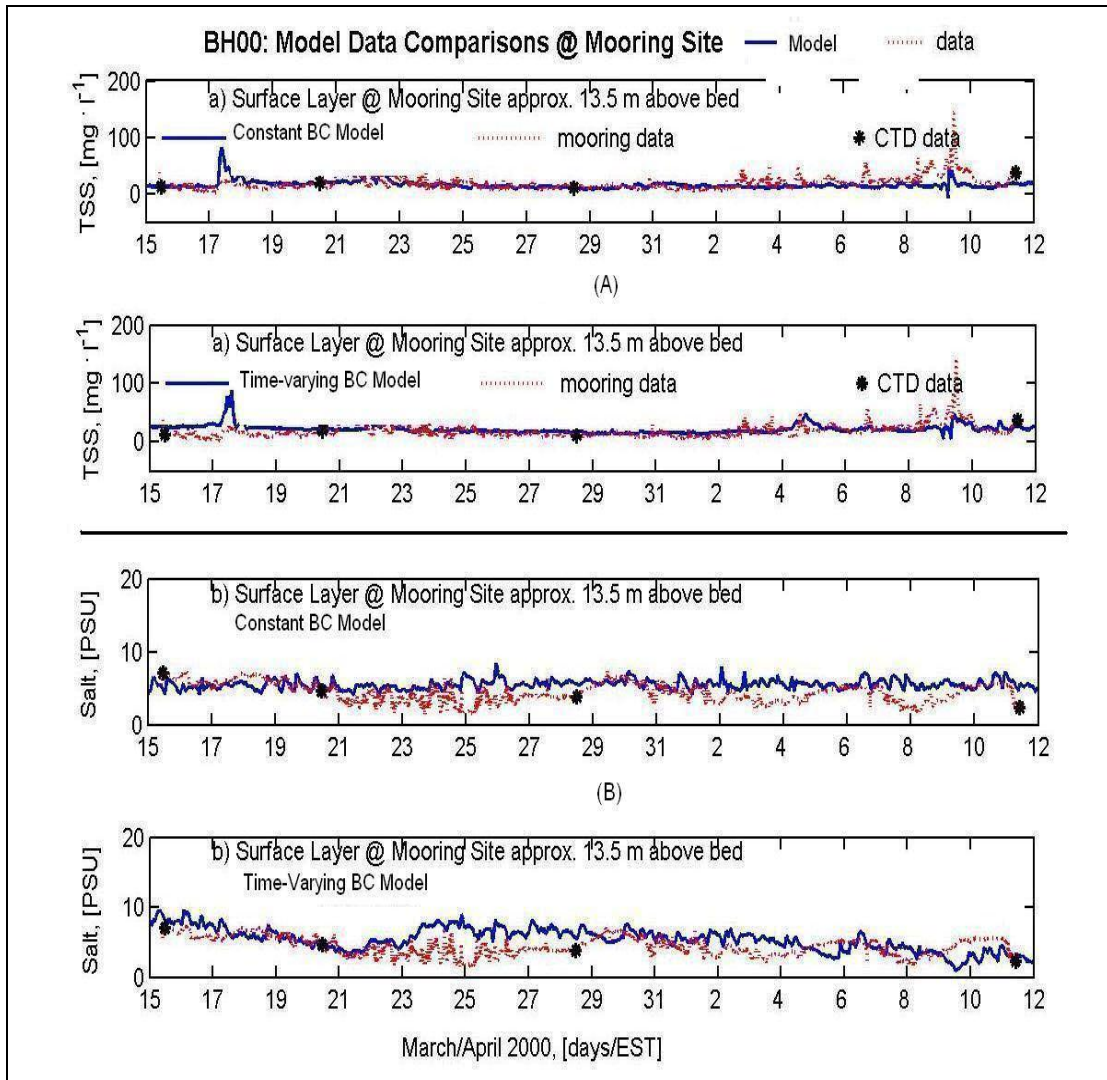


Figure 3.4.1: Model-data comparisons for TSS (A) and salinity (B) at mooring site 1 surface layer – CHARM 2

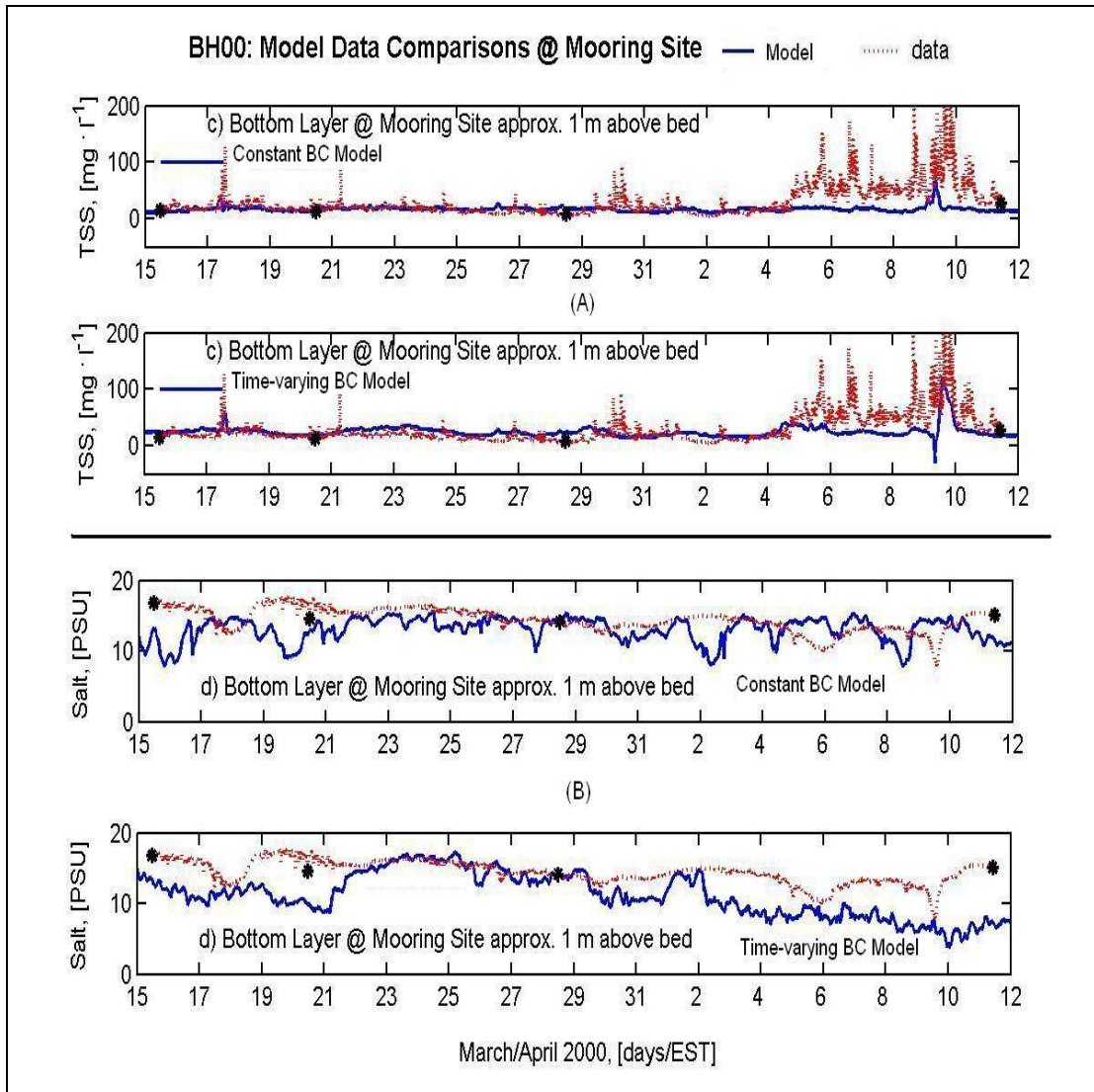


Figure 3.4.2: Model-data comparisons for TSS (A) and salinity (B) at mooring site 1 bottom layer – CHARM 2

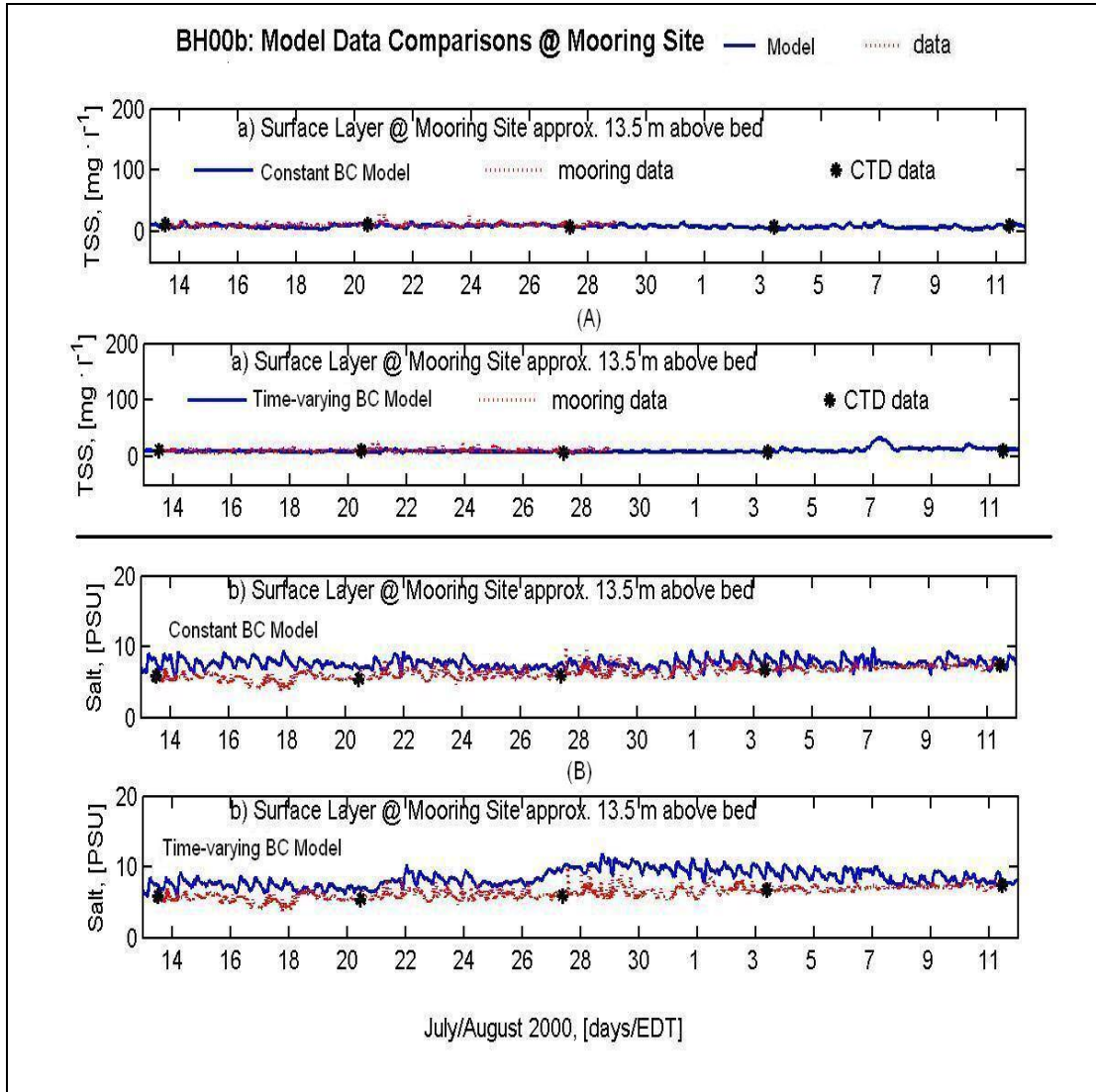


Figure 3.4.3: Model-data comparisons for TSS (A) and salinity (B) at mooring site 1 surface layer – CHARM 3

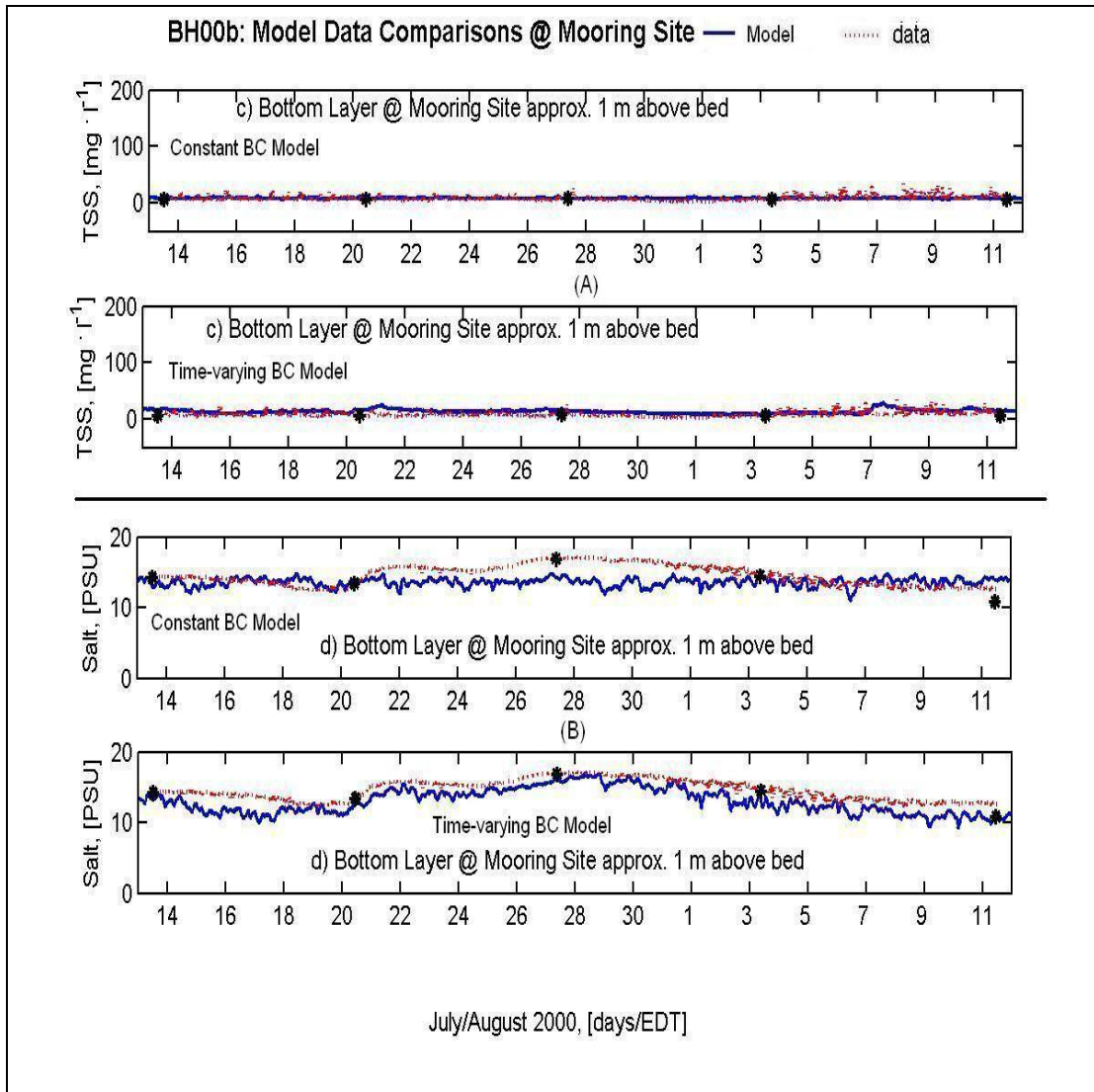


Figure 3.4.4: Model-data comparisons for TSS (A) and salinity (B) at mooring site 1 bottom layer – CHARM 3

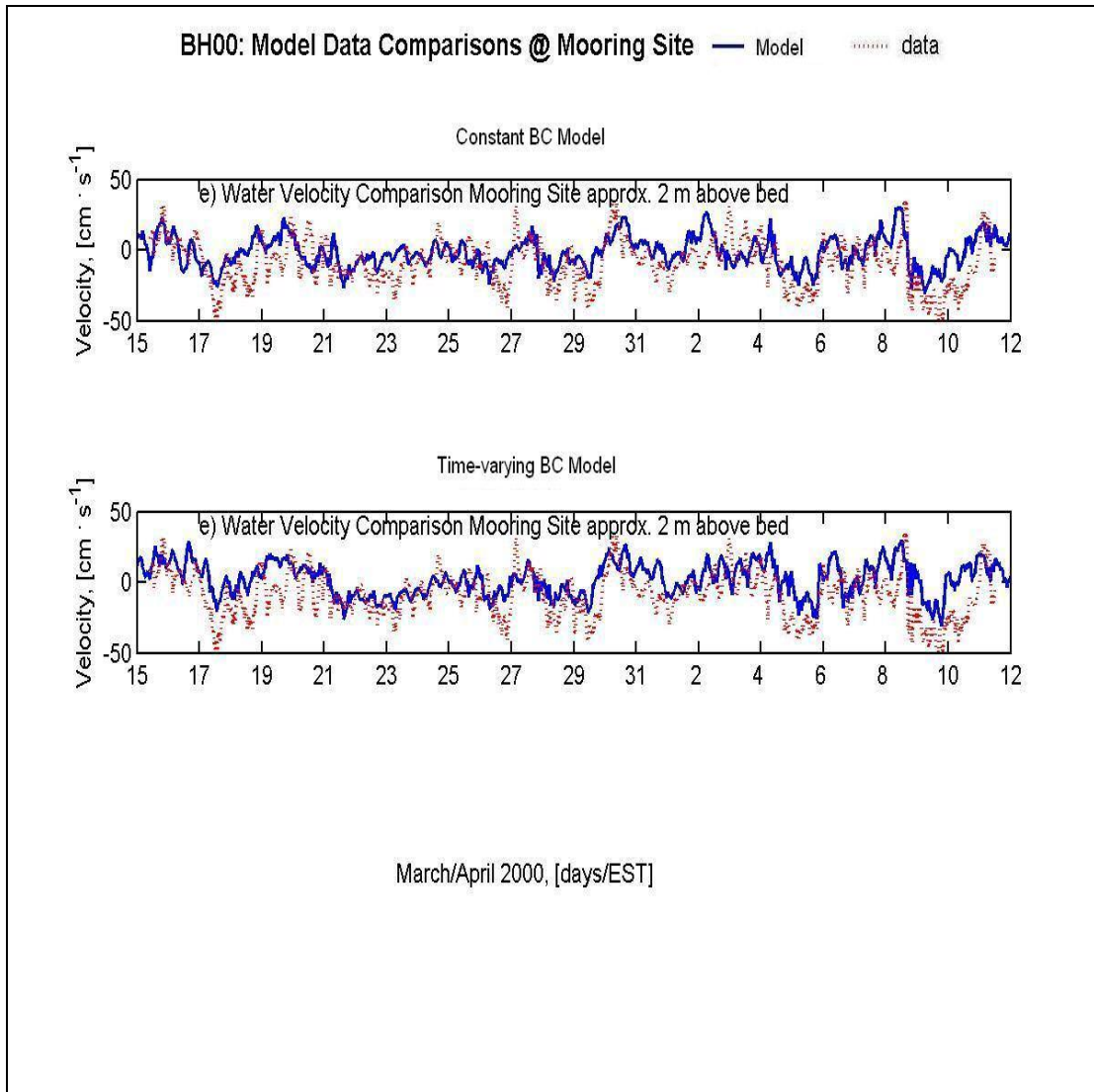


Figure 3.4.5: Model and data comparison of velocity at mooring site 1 bottom layer - CHARM 2

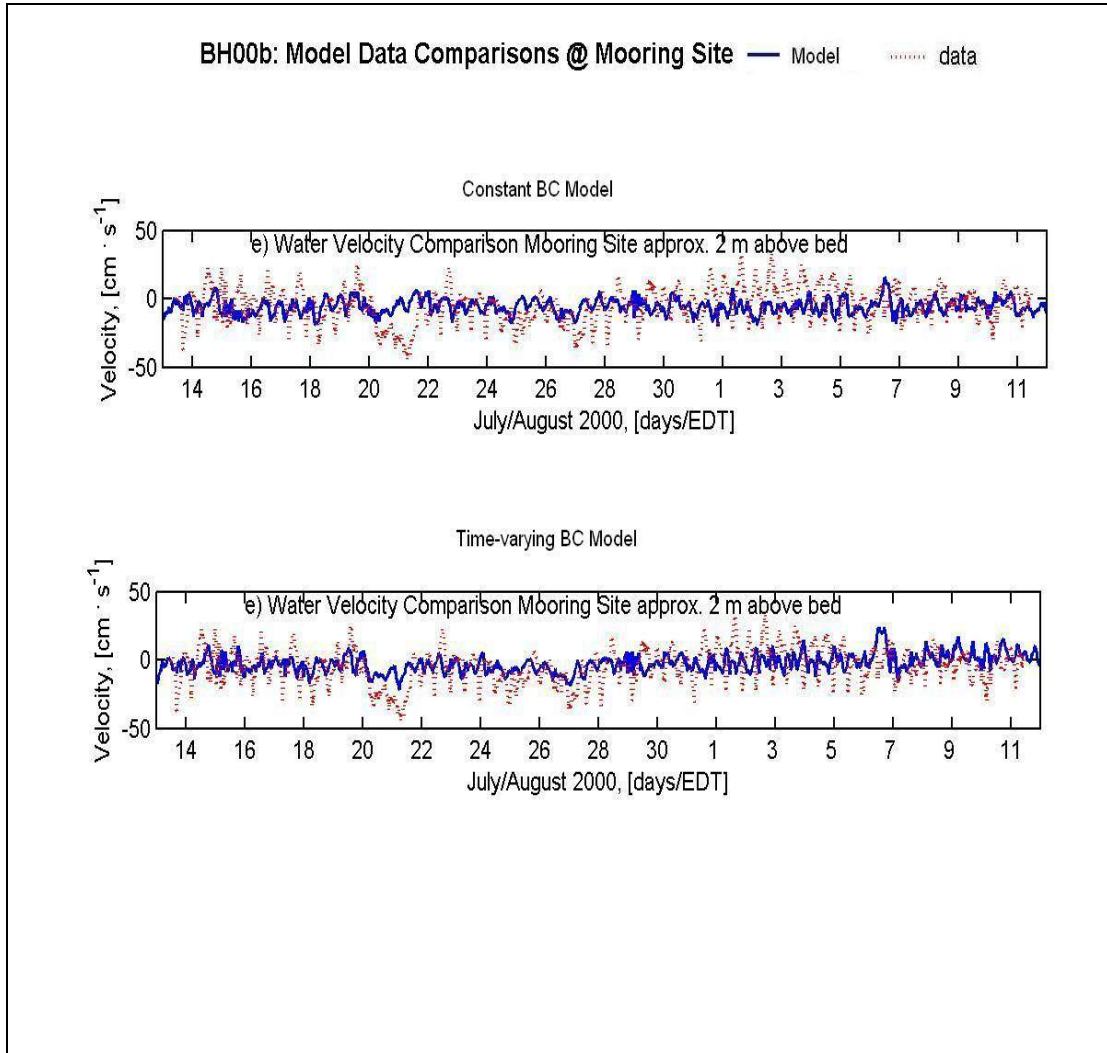


Figure 3.4.6: Model and data comparison of velocity at mooring site 1 bottom layer - CHARM 3

site 1 are summarized on Table 3.4.1. The mean values of TSS for CHARM 2 seem to be predicted better with the time-varying BC model, but salinity is not. For both CHARM 2 and CHARM 3 cases, the standard deviations of TSS under time-varying boundary conditions are larger than those under constant boundary condition and closer to those of observational data. For the variability of salinity at mooring site 1, it is hard to say which model prediction is better. For velocity at bottom layers at mooring site 1, the constant BC model gives better prediction for the mean value. The time-varying model predictions of velocity at bottom layer have more variability for both simulation periods than those predicted by constant BC model, with standard deviations of velocity for both cases are larger.

The comparisons of data and model predictions under two sets of boundary conditions at sampling site 2 are illustrated in Figure 3.3.7 to Figure 3.3.12 for salinity and sediment at surface, middle and bottom layers for CHARM 2 and CHARM 3 periods. The time series of model predictions under two sets of boundary condition are different. However, there are no time series of salinity and sediment data available for sampling site 2. Comparing to a few scattered CTD (conductivity, salinity and depth) data, the salinity and sediment predictions of both models seem reasonable and it is hard to say which model prediction has better agreement with observation.

Figure 3.4.13 to Figure 3.4.15 show comparisons between model axial velocity predictions under two sets of boundary conditions and measured ADCP velocities at mooring site 1 during CHARM 3 period, the only field period in which ADCP observations are available. Again, the time-series of model predicted velocities under

			Mean		
			Constant BC model	Data	Time-varying BC model
CHARM 2	surface	salinity	5.252	4.428	5.481
		tss	16.141	19.53	22.219
	bottom	salinity	12.921	14.495	11.104
		tss	16.612	28.297	25.814
	Velocity at bottom		-1.332	-9.08	1.405
CHARM 3	surface	salinity	7.589	6.314	8.423
		tss	8.959	10.942	11.106
	bottom	salinity	13.541	14.656	12.876
		tss	8.714	8.383	13.968
	Velocity at bottom		-5.853	-4.98	-2.642
			Standard Deviation		
			Constant BC model	Data	Time-varying BC model
CHARM 2	surface	salinity	1.679	1.293	0.631
		tss	6.719	12.503	7.104
	bottom	salinity	1.741	1.659	3.032
		tss	4.39	25.935	10.651
	Velocity at bottom		10.785	15.896	11.405
CHARM 3	surface	salinity	0.692	0.81	1.133
		tss	3.228	2.748	3.909
	bottom	salinity	0.619	1.442	1.82
		tss	0.966	3.905	3.45
	Velocity at bottom		5.549	12.867	6.663

Table 3.4.1: Mean values and standard deviations of salinity, TSS and Velocity at mooring site 1 for CHARM 2 and CHARM 3 periods

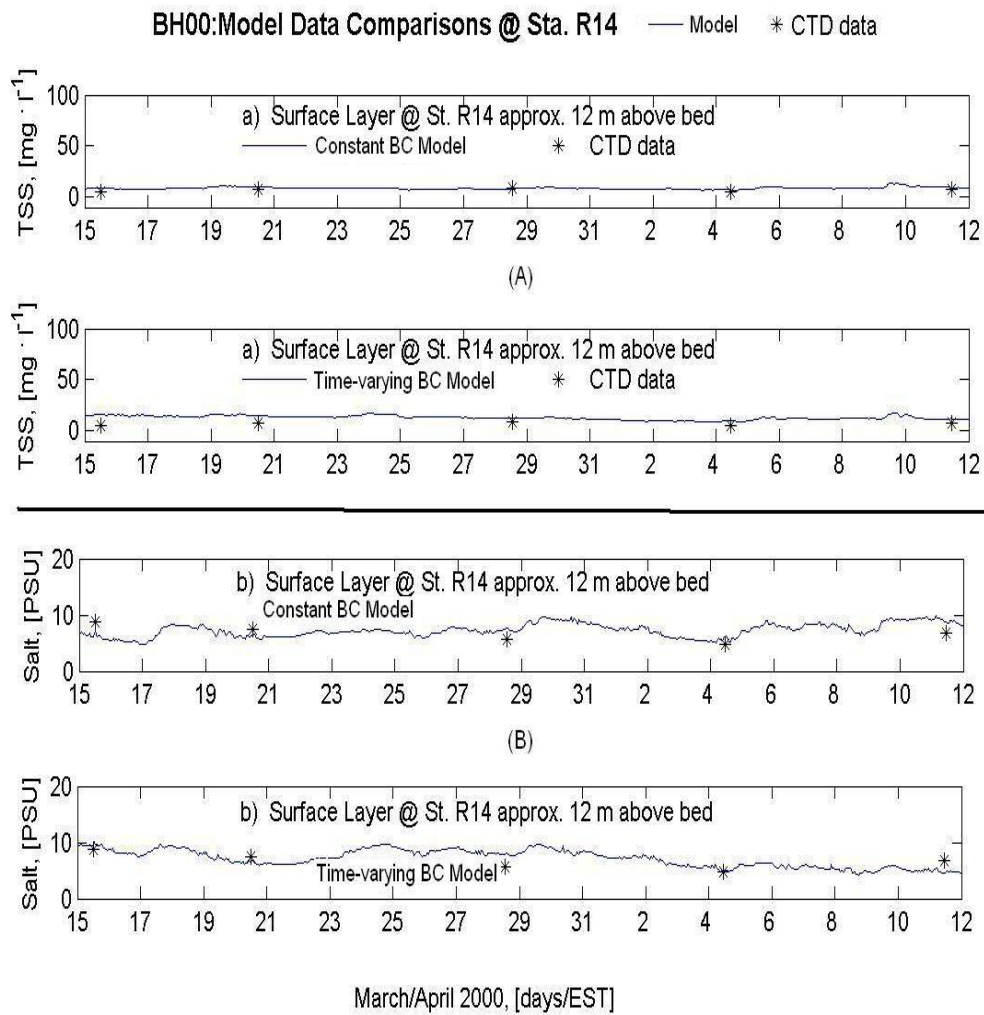


Figure 3.4.7: Model-data comparisons for TSS (A) and salinity (B) at sampling site 2 surface layer – CHARM 2

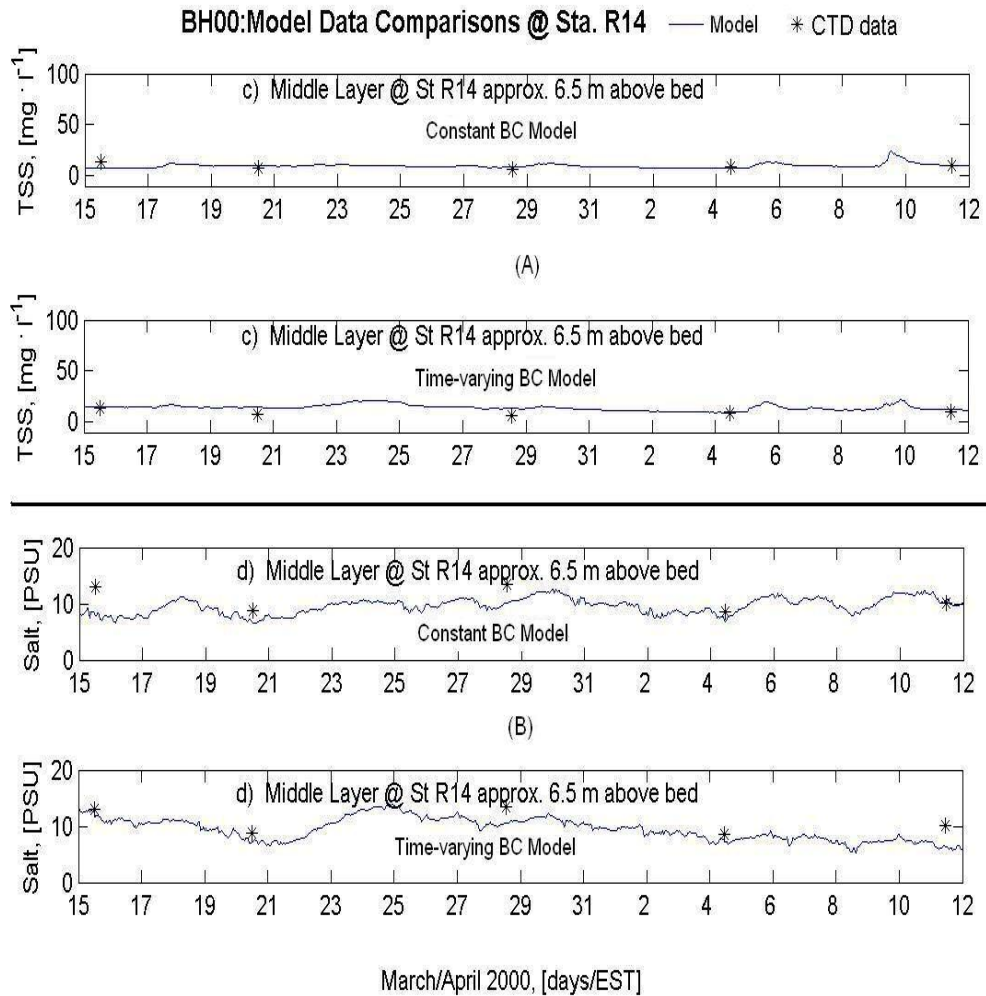


Figure 3.4.8: Model-data comparisons for TSS (A) and salinity (B) at sampling site 2 middle layer – CHARM 2

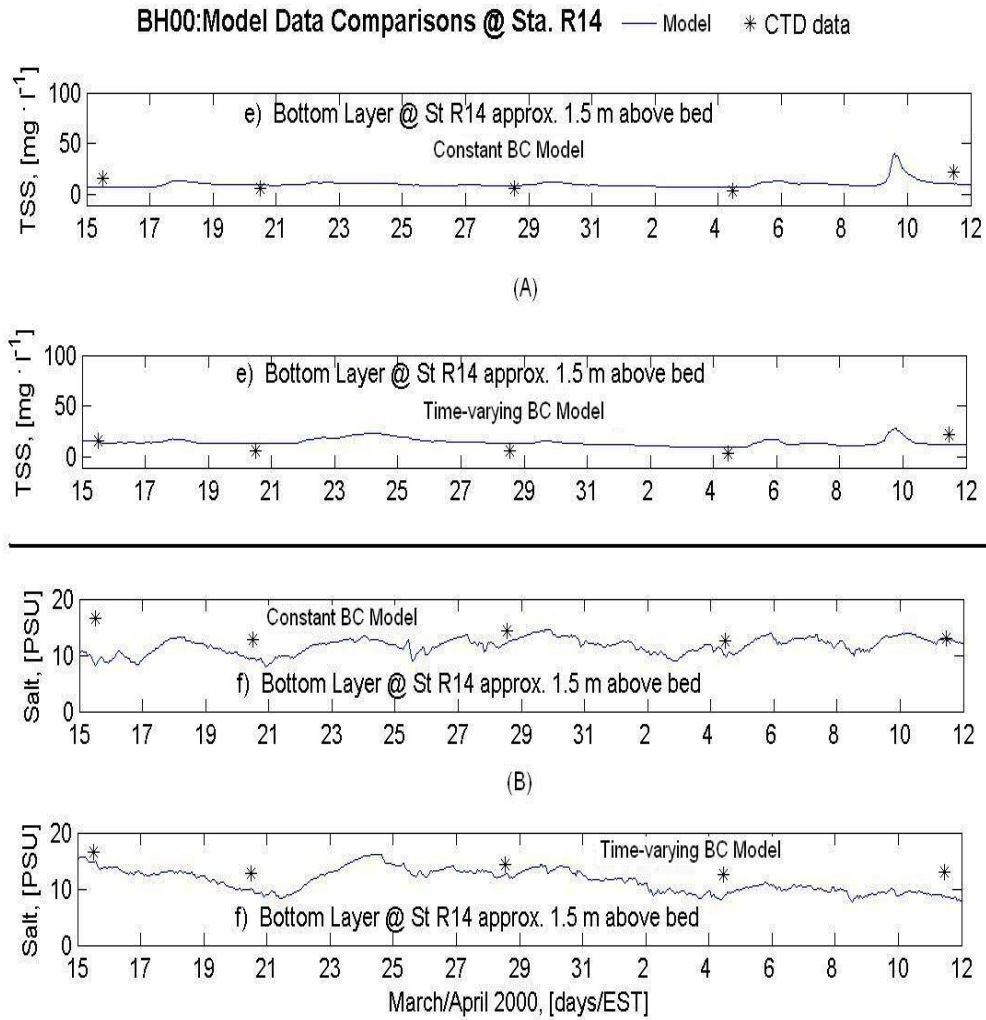


Figure 3.4.9: Model-data comparisons for TSS (A) and salinity (B) at sampling site 2 bottom layer – CHARM 2

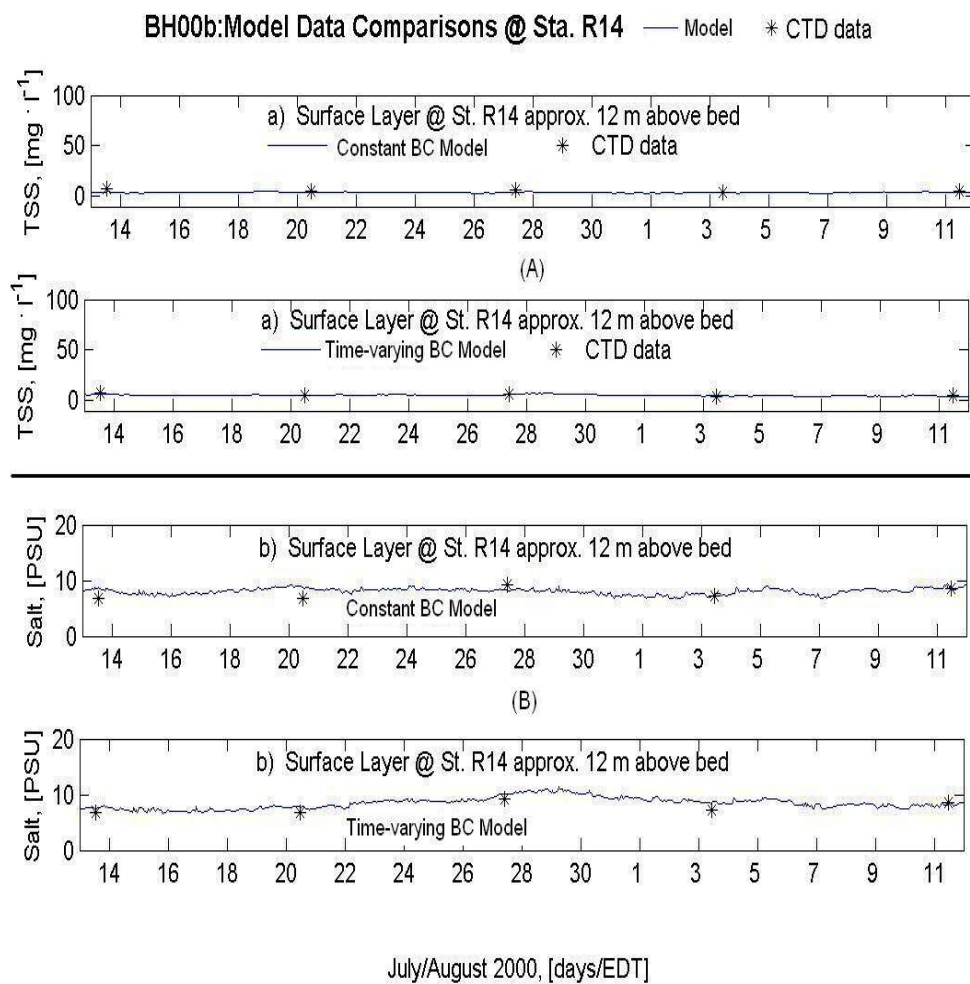
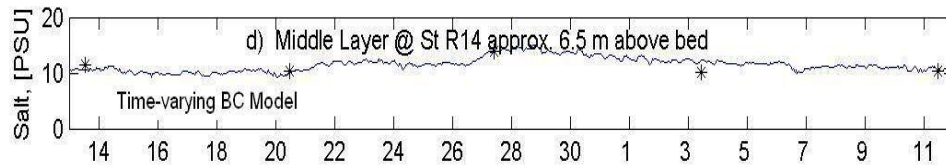
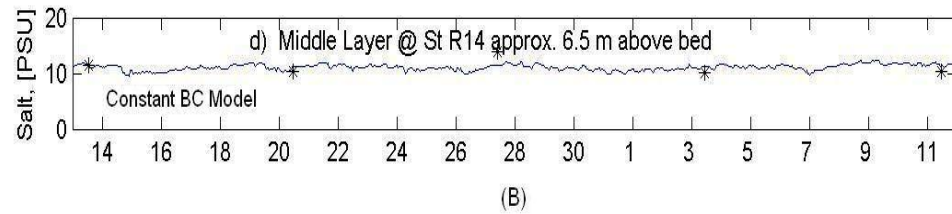
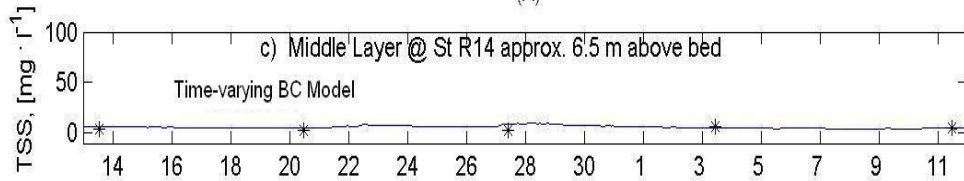
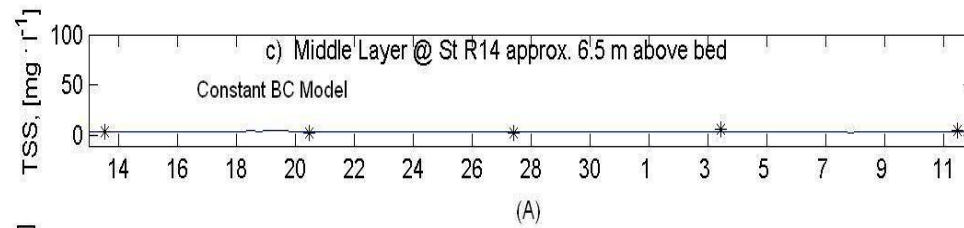


Figure 3.4.10: Model-data comparisons for TSS (A) and salinity (B) at sampling site 2 surface layer – CHARM 3

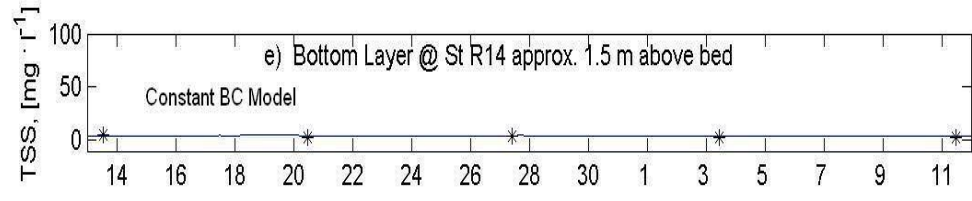
BH00b: Model Data Comparisons @ Sta. R14 — Model * CTD data



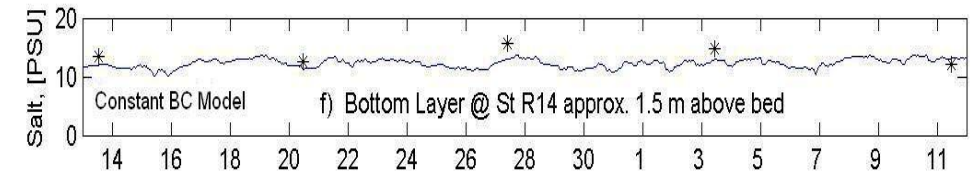
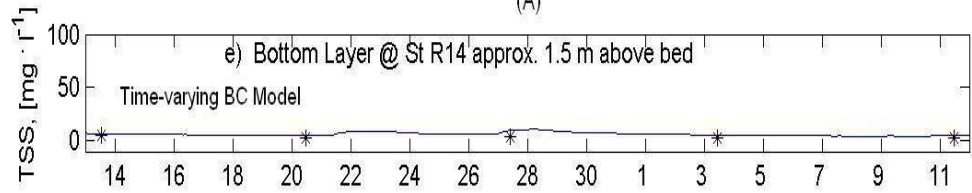
July/August 2000, [days/EDT]

Figure 3.4.11: Model-data comparisons for TSS (A) and salinity (B) at sampling site 2 middle layer – CHARM 3

BH00b:Model Data Comparisons @ Sta. R14 — Model * CTD data



(A)



(B)

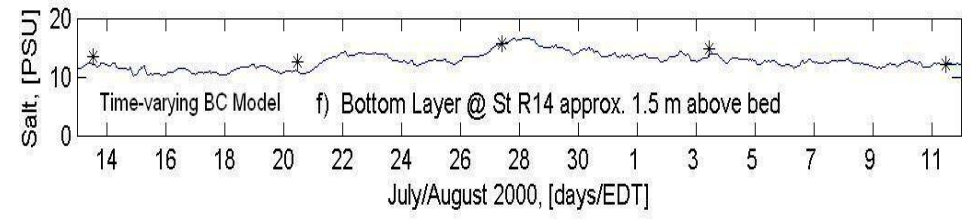


Figure 3.4.12: Model-data comparisons for TSS (A) and salinity (B) at sampling site 2 middle layer – CHARM 3

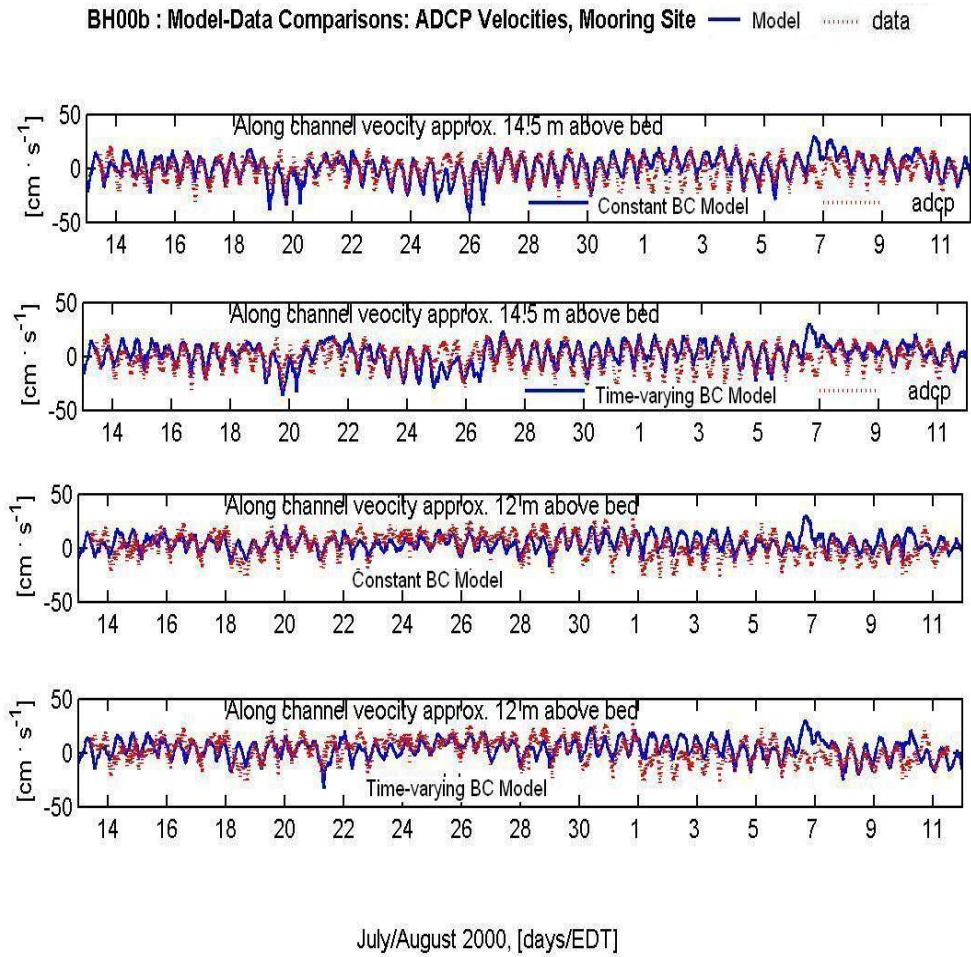


Figure 3.4.13: Model axial velocity - ADCP velocity comparison at mooring site 1 surface layer – CHARM 3

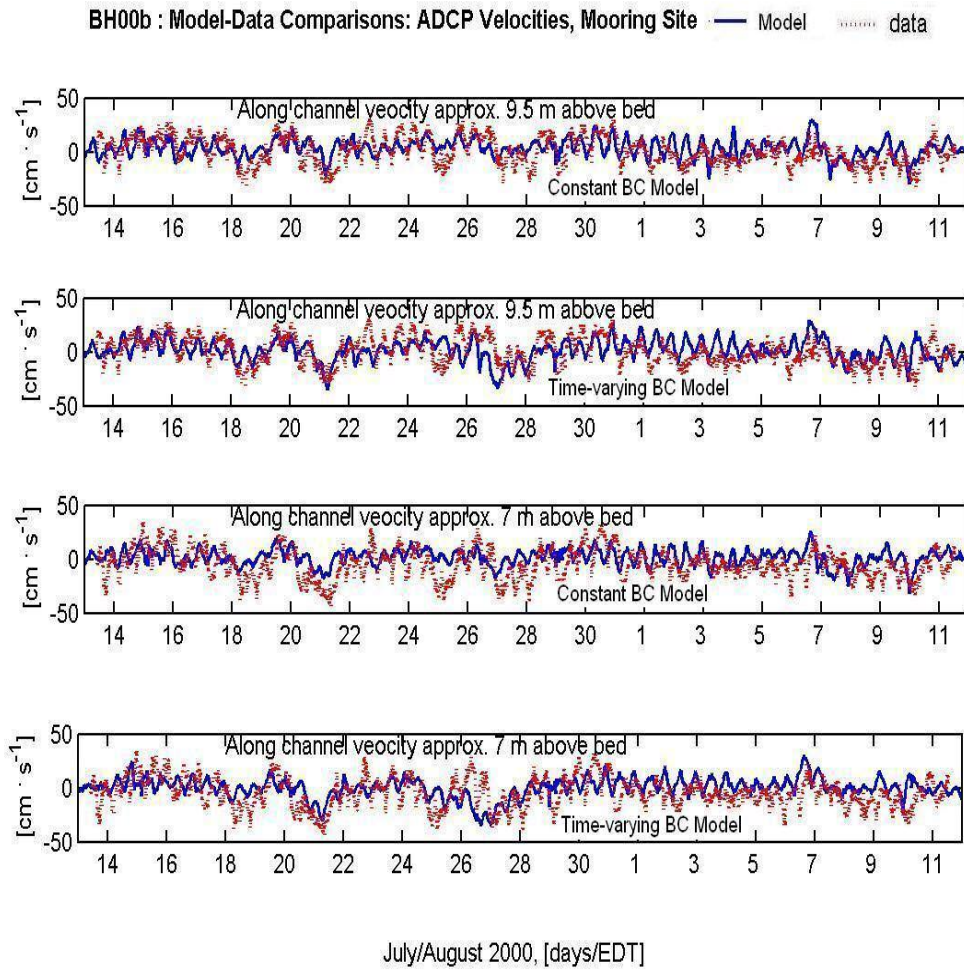


Figure 3.4.14: Model axial velocity - ADCP velocity comparison at mooring site 1 middle layer – CHARM 3

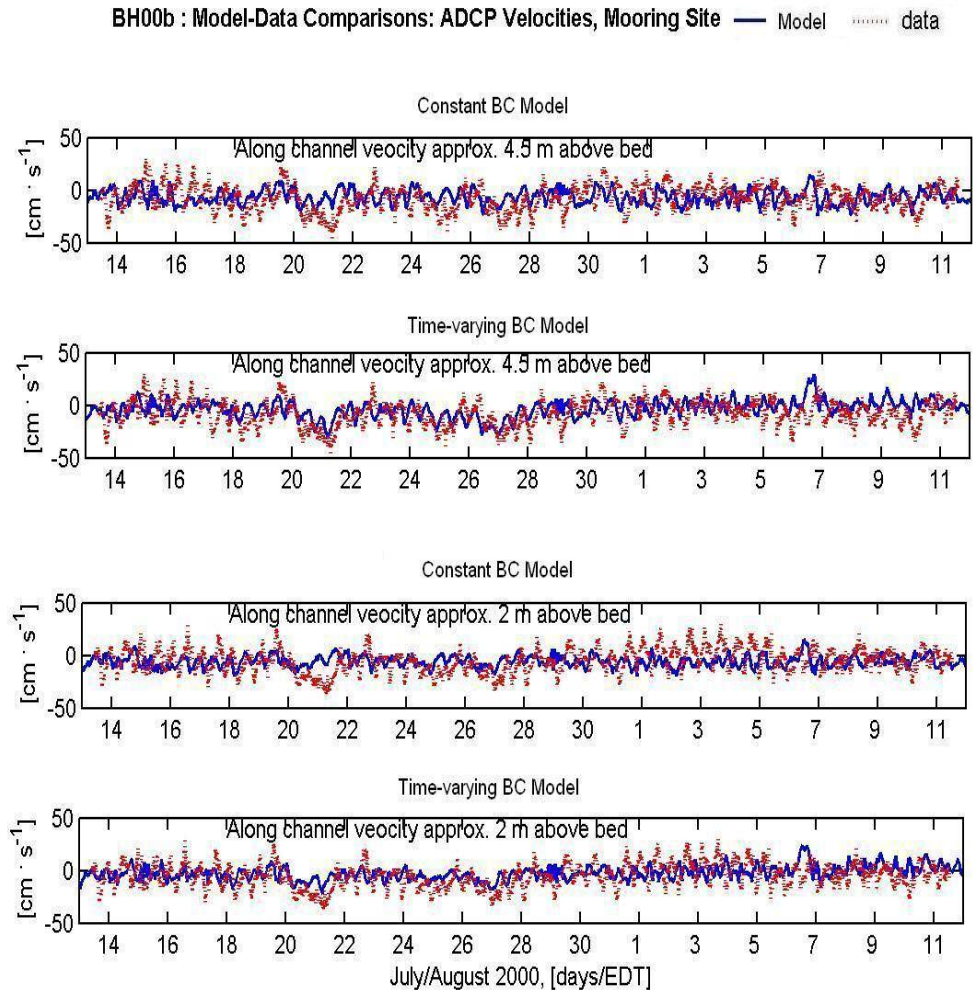


Figure 3.4.15: Model axial velocity - ADCP velocity comparison at mooring site 1 bottom layer – CHARM 3

both boundary conditions look different. The mean values and standard deviations of velocity data and model predictions are summarized in Table 3.4.2.

Figure 3.3.16 shows the mean vertical velocity profile of model prediction vs. ADCP (Acoustic Doppler Current Profiler) data at mooring site 1. For monthly-averaged velocities, two model predictions do not simulate the near surface velocity well. The ADCP data shows clearly three-layer circulation pattern with inflows in surface and bottom layers and outflow in the middle layer. However, the velocity predictions of both models are unable to show the surface inflows from the monthly averaged vertical velocity profile at mooring site 1. But the shears of mean vertical velocities under both sets of boundary conditions have the similar pattern with that of ADCP data. Comparing the two model results and data, the former model under constant boundary conditions seems to predict mean velocity better in the surface and bottom layers than the model prediction under time-varying boundary conditions. The time-varying BC model predictions capture the middle layer mean velocity better than the constant BC model. From the summary of standard deviation of velocity data and model predictions in Table 3.4.2, both model predictions underestimate the variability of velocity in the bottom layers. Overall, the time-varying BC model predictions show more variability than constant BC model predictions.

Also noticeable, there are interesting shifts between the mean vertical velocity of the ADCP data and model predictions under both boundary conditions (Figure 3.4.16). This shift might partially result from the difference between the real geometry and the model grid. Figure 3.4.17 shows the model bathymetry and real bathymetry derived from water

Model and ADCP velocity comparison at Mooring site 1- CHARM 3

	Velocity Mean		
	Constant BC Model	Data	Time-varying BC Model
14.5m above bed	0.61	-1.01	1.73
12m above bed	4.26	2.36	3.51
9.5m above bed	3.32	0.61	1.15
7m above bed	1.23	-4.75	-0.36
4.5m above bed	-6.88	-7.83	-3.83
2m above bed	-6.07	-5.32	-2.82
	Velocity Standard Deviation		
	Constant BC Model	Data	Time-varying BC Model
14.5m above bed	11.60	10.00	10.90
12m above bed	7.41	10.35	8.97
9.5m above bed	8.41	12.64	10.30
7m above bed	7.76	13.52	9.49
4.5m above bed	7.04	11.70	8.49
2m above bed	5.51	11.18	6.68

Table 3.4.2: Mean values and standard deviations of velocity at mooring site 1 for CHARM 3 Period

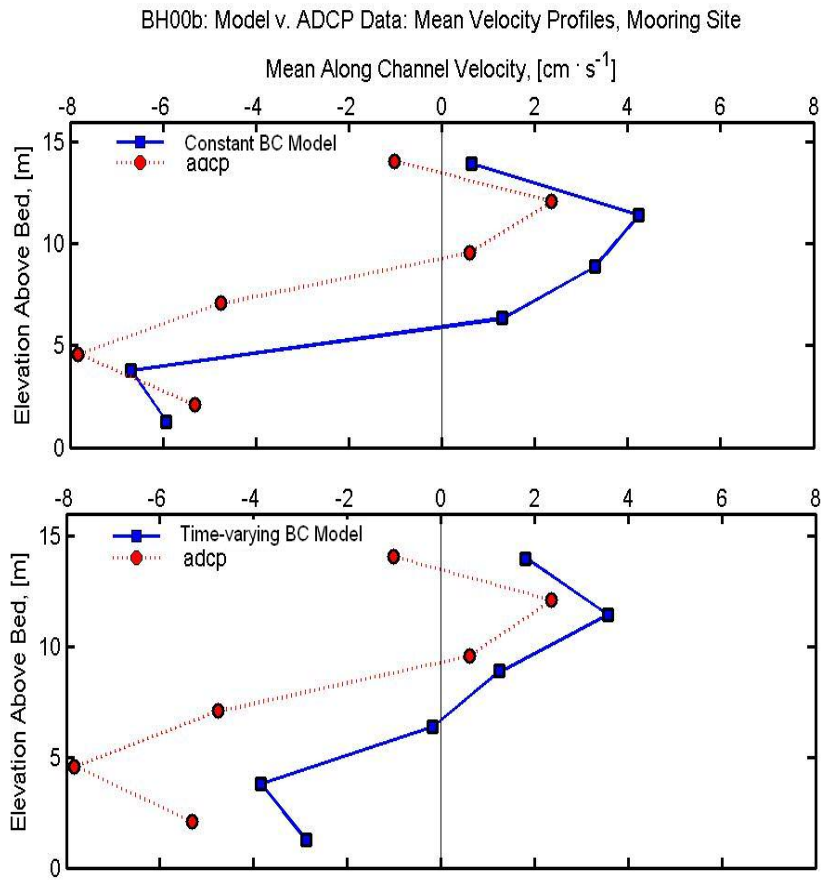


Figure 3.4.16: Mean velocity profiles at mooring site 1: Model predictions vs ADCP data

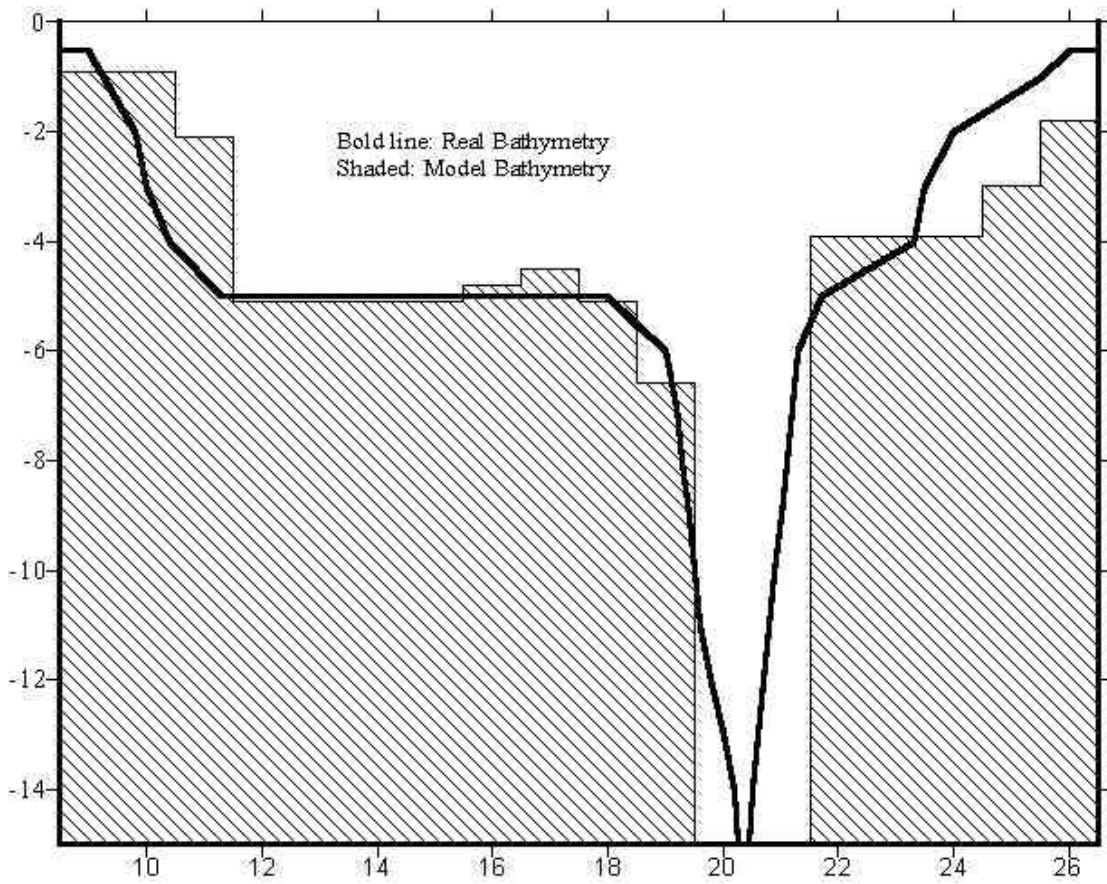


Figure 3.4.17: Model and real bathymetries at the cross section of Baltimore Harbor mouth

depth sampling data. It is clear that the bottom layer of the deep channel in CHARM model is wider than that of the real condition.

Chapter 4: Discussion and Conclusion

In theory, the interior solution of the domain of interest far from a boundary should not be subject to changes in open boundary conditions, but experience has shown that the interior solution can be overly sensitive to the specified open boundary conditions (Z. Li, 1999). In Baltimore Harbor, the interior is close to the open boundary at Harbor mouth. In most estuary models (e.g. Oey et al., 1985; Chao et al., 1996), the systems of interest are driven by open boundary density and sea level. In this study, the hydrodynamics and sediment transport in Baltimore Harbor are simulated using a three-dimensional CHARM model under two sets of open boundary conditions at the Harbor mouth. The constant monthly-averaged salinity and sediment boundary conditions are obtained from observational data (Sanford et al., 2003). The time-varying salinity and sediment boundary conditions are derived from CH3D model output (Lin et. al, 2004).

The results of this study confirm that open boundary conditions at Harbor mouth do have a strong effect on the model predictions in Baltimore Harbor (e.g. Figure 3.2.6). This is reasonable since Baltimore Harbor is a small estuary system. The total distance from Harbor head to mouth is only about 20 km. Also how far boundary-condition effects propagate into Baltimore Harbor is investigated in this study. In general, the boundary conditions have more effect on the model predictions at mooring site 1 than model predictions at sampling site 2 (Table 3.2.2). This is consistent with the fact that mooring site 1 is much closer to the open boundary at Harbor mouth than sampling site 2. Also, the salinity differences under two sets of boundary conditions do not decrease much

(less than 30%) from mooring site 1 to sampling site 2 (Table 3.2.2). Remember, the distance between mooring site 1 and sampling site 2 is about 10 km, which is about half of the length of Baltimore Harbor. The results indicate that the boundary condition effects on salinity propagate efficiently along deep channel and salinity differences drive the circulation. This probably is because salt moves completely with water and the horizontal transport of water is dominant compared to vertical water transport in this study. However, for sediment, it is not the same situation. The suspended sediment concentration differences under two sets of boundary conditions decrease a lot (more than 50%) from mooring site 1 to sampling site 2 (Table 3.2.2). This is due to the characteristics of sediment transport. Vertical sediment transport is always dominant in sediment transport of this study (Table 3.3.1 and Table 3.3.2). Compared to salinity, the boundary condition effects on suspended sediment concentration do not propagate as far along the deep channel because there is always a strong tendency for sediment to settle down nearby.

One of the key standards to judge if a model functions well is that if the model can achieve stable, mass conservative solutions. The sediment mass-balance results under either boundary conditions are good for both CHARM 2 and CHARM 3 simulation periods (Table 3.3.1 and Table 3.3.2), with error less than 1.3%. These results prove that models under both open boundary conditions are configured well to keep sediment mass balance in Baltimore Harbor. The mass balance results under time-varying BC model are even better with error less than 0.2%. This result might be because the time-varying boundary condition is closer to real boundary condition than constant boundary conditions.

Comparing the sediment flux across Harbor mouth boundary in mass balance calculation under both boundary conditions (Table 3.3.1 and Table 3.3.2), it is obvious that boundary flux under time-varying boundary condition is larger (doubled for CHARM 3 case) in all cases. This means that more sediment is imported from the adjacent main Chesapeake Bay through the open boundary at the Harbor mouth under time-varying boundary conditions than under constant boundary conditions. This behavior seems reasonable because the time-varying boundary conditions indicate a tidal “pumping effect”. The time-varying boundary conditions capture events, but constant boundary conditions do not. Under time-varying boundary conditions, there is more wave action in the adjacent open Bay than inside the Harbor. Thus, there is more resuspended sediment in the water outside the Harbor, which results in more sediment imported from the adjacent Bay with the inflows. However inside the Harbor, with less wave action, the imported sediment tends to settle down in the bottom, and thus less suspended sediment is transported to the adjacent Bay with the outflows. Therefore, more sediment with flood tides and less sediment with ebb tides result in the net “pumping” of sediment from the adjacent Bay to the Harbor under time-varying boundary conditions. For the CHARM 2 case, the boundary flux (positive value) imports sediment from outside Harbor under time-varying boundary condition. However, the boundary flux under constant boundary condition (negative value) indicates the Harbor loses sediment to the adjacent bay in this case. All the boundary flux results under time-varying boundary conditions are consistent with the findings of Sinex and Helz (1982) that the Harbor imports fine sediment from the adjacent Chesapeake Bay and Lin et al.

(2004) that the major sediment source in Baltimore Harbor comes from outside the Harbor, especially from the Susquehanna.

Suspended sediments in the water column are transported with the water through advection and diffusion. In addition, suspended sediment could be exchanged from water column to bottom sediment through deposition. Deposition is driven by gravity and the rate of deposition depends on the characteristics of the sediment and the flow regime. Sediment also could be transported from the sediment surface to water column through erosion/resuspension. Erosion or resuspension of bottom sediment is one of the major sources for total suspended sediment (TSS) in water column. The erosion rate varies with the energy available for erosion, from bottom shear, and the characteristics of the sediments (Sanford et al., 1997; Chang, 1999). It is easy to understand that the time-varying boundary conditions could make the water more dynamic and bring more variability to water system than the constant boundary conditions. The more dynamic water system brings more energy for erosion. From the sediment boundary flux through mouth, we know that more fine sediment is imported from adjacent bay under time-varying boundary conditions. These two aspects explain why there is more suspended sediment in water column under time-varying boundary conditions for both CHARM 2 and CHARM 3 simulation periods (Table 3.3.1 and Table 3.3.2). More suspended sediment in water column makes more sediment deposition for these simulation cases under time-varying boundary conditions (Table 3.3.1 and Table 3.3.2). Sediment erosion under time-varying boundary condition increases for the CHARM 2 period, but change very little in the CHARM 3 period (Table 3.3.1 and Table 3.3.2). This result may be because CHARM 2 is a high wind spring period and CHARM 3 is a calm, low wind

summer period. The energy from the time-varying boundary condition is not sufficiently strong to make more sediment eroded from the bottom for the calmer CHARM 3 period. So compared to effects of wind, tides, wave and current, the effect of open boundary conditions on the vertical sediment transport is secondary in Baltimore Harbor. This conclusion is also indicated by the sediment predictions, which do not change much under these two different sets of boundary conditions, and by the vertical sediment transport (erosion/deposition), which is dominant in sediment transport in all simulation cases of this study.

The constant BC model is a reasonable predictor of large scale, monthly averaged transport of water and sediment in Baltimore Harbor, but it does not do as good a job at predicting short-term, small-scale variability (Sanford et al., 2003). So this study modifies the CHARM model used in the study of Sanford et al. (2003) by adopting time-varying salinity and sediment concentration boundary conditions at Harbor mouth to try to improve the short-term model predictions. After comparing the model predictions of salinity, TSS and velocity under two sets of boundary conditions with observational data for both CHARM 2 and CHARM 3 periods (Figure 3.4.1 to Figure 3.4.16), we find that, in general, the short-term model predictions under both boundary conditions are not in very good agreement with observational data. This result is partially because both boundary conditions are not accurate simulations of actual condition. Also, the grid system used in CHARM model has some numerical limitations, which might play a role in the short-term model predictions. The CHARM model “stair-step” grid causes resistance for the water and sediment transport. So the model predictions might get improved if adopting more realistic curvilinear coordinate.

For the monthly averaged values, both model predictions of salinity and sediment concentration are reasonable, compared to observational data at mooring sites 1 and sampling site 2. Since the constant boundary conditions are the monthly averaged values interpolated from observational data near Harbor mouth, they are consistent with the good model monthly averaged predictions under this kind of boundary conditions (Sanford et al., 2003). For time-varying BC model, the model gets reasonable monthly averaged predictions because the CH3D model outputs used to derive the time-varying boundary salinity and TSS values are calibrated with observational data (Lin et al., 2004).

However, the time-varying BC model does not improve the short-term predictions much as expected when we carefully look into the time-series of model predictions and observations (Figure 3.4.1 to Figure 3.4.16). The salinity, sediment and velocity predictions of time-varying BC model do have more variability at mooring site 1 in all cases (Table 3.4.1 and Table 3.4.2) than those of constant BC model. This is consistent with the fact that the time-varying boundary condition itself brings more variability and mooring site 1 is close to Harbor mouth boundary. But a lot of short-term variability in observational data does not appear in the model results at mooring site 1, especially for the near bottom sediment concentration predictions. This is partially because the model does not considering shipping activity in the deep channel along Baltimore Harbor, which is possibly responsible for the brief large spike of sediment concentration data at the bottom layers (Sanford et al., 2003). Also, even though the time-varying boundary conditions are derived from the calibrated CH3D model output, the time-series values used as boundary condition are still different from real observational data. As seen in Table 3.2.1, the mean values of sediment concentrations used in boundary cell (51,21) are

not similar to the constant sediment concentrations of the same cell under constant boundary condition model which are the monthly averaged values of real observational data near Harbor mouth. So the time-series values used as time-varying boundary conditions must differ from real observational data, especially for the sediment concentration at the bottom layers along the deep channel at Harbor mouth.

The Harbor often experiences the unique three-layer residual circulation (Boicourt and Olson, 1982). The Freshwater input from the upland is very limited, hence the freshet from Susquehanna River often brings fresher water into the Harbor from the mouth of the Harbor. Thus, fresh and dense saline water flows from the Bay into the Harbor at the surface and bottom, respectively, while the intermediate density water flows out of the Harbor in the mid-depth of the water column. From the CHARM observations (Baker et al., 2002), the three-layer circulation in Baltimore Harbor is a persistent but weak feature, and it is highly modulated by a stronger wind forced circulation, which is in agreement with Boicourt and Olson (1982). The model predictions of the mean vertical velocity profiles at mooring site 1 under both boundary conditions for CHARM 3 period do not show the inflow in the surface layer (Figure 3.4.16) as shown in ADCP velocity data. CHARM 3 is a calm mid-summer period with low wind and low flow from Susquehanna River, so we expect the surface inflow would be very shallow, which could be seen from the ADCP data. Since the shear of the mean vertical velocity is similar to that of data and the surface inflow layer is always shallow (Boicourt and Olson, 1982), especially for the CHARM 3 period, perhaps this problem could be solved by dividing more layers in the vertical and thus make each vertical layer more thinner. By doing so, the model simulation time step should be shortened, too, for the purpose of model stability.

There are shifts between the mean ADCP velocity profile and those of model predictions under both sets of boundary conditions (Figure 3.4.16). Several reasons might cause this phenomenon. First, as mentioned before, the under-predicted bottom velocity might result from the wider bottom layer in the model grid (Figure 3.4.17). Second, the model is constrained by continuity to keep mass balance. Third, the ADCP data showing in Figure 3.4.16 is only for one sampling site, which is located at the northside of the deep channel. The ADCP data is an Eulerian velocity mean and does not represent the whole cross-section mean velocity profile at the deep channel. If examining the ADCP mean vertical velocity carefully, you will find the inflow is bigger than outflow in this case. Clearly, if this represents the cross-section average velocity, then Harbor would be quickly flooded. So in order to improve the model-data comparison, more spatial sampling data is needed.

In summary, this study tried to improve the short-term predictions of CHARM hydrodynamic and sediment transport model in Baltimore Harbor by using time-varying salinity and sediment boundary conditions at Harbor mouth. The models do have different, but reasonable predictions corresponding to two different boundary conditions at Harbor mouth. However, the short-term predictions do not get as much improvement under the time-varying boundary conditions as expected. Thus, if this CHARM model were to improve the short-term predictions of sediment transport in future study, there are several factors should be considered:

1. using the real observational time-series data at Harbor mouth as boundary conditions;
2. considering the shipping activities in deep channel;

3. getting more spatial and longer period of data at Harbor mouth and inside Harbor, especially along the deep channel;
4. refining the model vertical grid;
5. changing the model grid system to more realistic one like curvilinear grid system.

And if the only concern is the monthly averaged predictions, then maybe the constant BC model is good enough and economically feasible.

References

- Baker J., et al., 2002. Final Report: Comprehensive Harbor Assessment and Regional Modeling Study. Part 1: Field Study.
- Boicourt W.C. and P. Olson, 1982. A Hydrodynamic study of the Baltimore Harbor System. Tech. Rep. 82-10, Chesapeake Bay Institute, The Jones Hopkins University, 131pp.
- Chang, M-L., 1999. Modeling the Effect of Resuspension and Deposition on Early Diagenesis of Nutrients and Contaminants. University of Maryland, College Park, MD, 233pp.
- Chao, S.Y. and Wu, S.Y., 1995. Sparrows Point shoreline reclamation project: Hydrodynamic model of Baltimore Harbor. UMCEES, Horn Point Environmental Laboratory, Cambridge, MD, 118pp.
- Chao, S.-Y., W.C. Boicourt and H.V.C. Wang (1996). Three-layered circulation in reverse estuaries. *Continental Shelf Research* 16(10): 1379-1397.
- Chao, S. Y. Hyperpycnal and buoyant plumes from a sediment-laden River. *J. of Geophysical Research*, Vol. 103-c2, p3067-3081, 1998.
- Garland, C.F., 1952: A study of Water Quality in Baltimore Harbor. Maryland Board of Natural Resources. Publ. No. 96, 132pp.
- Greer, J. and Terlizzi, D., 1997. Chemical Contamination in Chesapeake Bay. Maryland Sea Grant, College Park, MD, 210pp.
- Knudsen, M., 1901: Hydrographical Tables. G.E.C.Gad, Copenhagen, Williams and

Norgate, London.

Li, Zhen, 1999. Responses of Estuarine Circulation to Vertical Mixing, River Inflow, and Wind Forcing. University of Maryland, College Park, MD., 234pp.

Lin, Jing, Harry Wang, G. M. Sisson, and Jian Shen (2004). Toxic Modeling in an Industrial Harbor -- a Case Study for Baltimore Harbor. Proceeding of the 8th International Conference, ASCE Estuarine and Coastal Modeling, edited by M. L. Spaulding. P455-474.

Maa, J.P.-Y., Sanford, L.P. and Halka, J.P., 1998. Sediment Resuspension characteristics In Baltimore Harbor, Maryland. Marine Geology, 146:137-145.

Maryland Department of the Environment, 1996. Toxics Regional Action Plan for Baltimore Harbor. Maryland Department of the Environment, Baltimore, MD, 230pp.

Mellor, G.L. and T. Yamada, 1982: A three-dimensional, primitive equation numerical ocean model. Atoms. and Oceanic Sciences Program, Princeton Univ., 44pp.

Nakagawa, Y., Sanford, L.P. and Halka, J., 2000. Effect of wind waves on distribution of Muddy bottom sediments in Baltimore Harbor, USA. In: B.L. Edge (Editor), Coastal Engineering 2000: Proceedings of the conference. ASCE, Sydney, Australia, pp. 3516 –3524.

Oey L.Y., G.L. Mellor and R. I. Hires (1985). A Three-Dimensional Simulation of the Hudson-Raritan Estuary. Part I: Description of the Model and Model Simulations. Journal of Physical Oceanography, 15, 1676-1692.

- Pritchard D. W. and J. H. Carpenter (1960). Measurements of turbulent diffusion in estuarine and inshore waters. *Bulletin International Association of Science of Hydrology*, 20, 37-50.
- Sanford, L. P., 1994. Wave forced erosion of bottom sediments in upper Chesapeake Bay. *Estuaries*, 17(1B): 148-165.
- Sanford, L.P., Chao, S.-Y., et al., 1997. Sediment transport in Baltimore Harbor. Draft final report to Maryland Department of the Environment. UMCES, HPL, Cambridge, MD, 130pp.
- Sanford, L.P., Chao, S.-Y., et al., 1999. Development of a Contaminant Transport Model for Baltimore Harbor, Draft report to Maryland Department of the Environment, University of Maryland ,CEES, Horn Point Laboratory, Cambridge, MD.
- Sanford, L.P. and Maa, J.P.-Y., 2001. A unified erosion formulation for fine sediments. *Marine Geology*, 179(1-2): 9-23.
- Sanford, L.P. et al., 2003. Comprehensive Harbor Assessment and Regional Modeling Study, Draft final report to Maryland Department of the Environment, University of Maryland ,CEES, Horn Point Laboratory, Cambridge, MD.
- Sinex, S.A. and Helz, G.R., 1982. Entrapment of Zinc and Other Trace Elements in A Rapidly Flushed Industrialized Harbor. *Environ. Sci. Technol.*, 16: 820-825.